

# Supporting Information for

## Fluorogenic D-amino acids enable real-time monitoring of peptidoglycan biosynthesis and high-throughput transpeptidation assays

Yen-Pang Hsu, Edward Hall\*, Garrett Booher\*, Brennan Murphy\*, Atanas D. Radkov, Jacob Yablonowski, Caitlyn Mulcahey, Laura Alvarez, Felipe Cava, Yves V. Brun<sup>†</sup>, Erkin Kuru<sup>†</sup>, Michael S. VanNieuwenhze<sup>†</sup>

<sup>†</sup> Corresponding author

\*Contributed equally

Correspondence to: [mvannieu@indiana.edu](mailto:mvannieu@indiana.edu), [ekuru@uemail.iu.edu](mailto:ekuru@uemail.iu.edu), [ybrun@indiana.edu](mailto:ybrun@indiana.edu)

The data that support the findings of this study are available from the corresponding author upon reasonable request

### Table of Content

SI-Synthesis.....	2
SI-Methods of data acquisition.....	5
SI-Discussions.....	8
SI-Figures.....	11
SI-NMR spectra.....	23
SI-Table.....	33
SI-References.....	34

## SI-Synthesis

**Characterization systems and software for RfDAA synthesis.** NMR data was collected using Varian 500 MHz or 400 MHz NMR system controlled by Agilent Vnmr J (version 2.2D). The data was analyzed using MestReNova (Version 9.0.1-13254). HPLC data was collected using Hewlett Packard Series 1100 controlled by Agilent ChemStation For HPLC (Version B.04.03-SP1). MS data was collected using Agilent 1200 HPLC-6130 MSD system controlled by Agilent ChemStation for LC/MS (Version C.01.05).

### **Methyl 3-(3,4-dihydroquinolin-1(2H)-yl)propanoate (1)**

The following procedure was adapted from previously published literature<sup>1</sup>. To a 250 mL round bottom flask containing trifluoroethanol (TFE, 38 mL, 1 M) was added 1,2,3,4-tetrahydroquinoline (4.71 mL, 37.54 mmol), methyl acrylate (10.2 mL, 112.62 mmol, 3 equiv.), and a stir bar. The reaction mixture was stirred at 100 °C for 16 h. The solvent and methyl acrylate leftover were removed by distillation at 130 °C. The resulting crude product (7.8 g, 35.6 mmol, ~95% yield, light-yellow oil) was carried onto the next reaction without further purification. <sup>1</sup>H NMR (400 MHz, Chloroform-*d*) δ 7.04 (t, *J* = 7.8 Hz, 1H), 6.94 (d, *J* = 7.4 Hz, 1H), 6.58 (d, *J* = 7.6 Hz, 2H), 3.68 (d, *J* = 1.4 Hz, 3H), 3.60 (t, *J* = 7.3 Hz, 2H), 3.27 (t, *J* = 5.6 Hz, 2H), 2.73 (t, *J* = 6.5 Hz, 2H), 2.64 – 2.55 (m, 2H), 1.93 (p, *J* = 6.1 Hz, 2H); ESI MS [M+H] 248.1.

### **3-(6-formyl-3,4-dihydroquinolin-1(2H)-yl)propanoic acid (2)**

The following procedure was adapted from previously published literature<sup>1</sup>. To a 250 mL round bottom flask was added **1** (8.23 g, 37.4 mmol), DMF (29 mL, 374 mmol, 10 equiv.), dichloromethane (74.8 mL, 0.5 M), and a stir bar. The reaction was cooled down to freezing point in an ice bath. Phosphoryl chloride (7 mL, 74.8 mmol, 2 equiv.) was then added to the reaction drop by drop with continuous stirring. The reaction was stirred on ice bath for 2 h. The resulting product was extracted with 100 mL dichloromethane and washed sequentially with 1M sodium hydroxide solution twice, 10% copper (II) sulfate solution (w/w) once, brine solution twice, and dried over magnesium sulfate. The crude product was purified using column chromatography (3:7 EtOAc/Hexane) to provide non-colored oil product (6.59 g, 26.7 mmol, 71% yield). The purified product (6.59g, 26.7 mmol) was then added to a 100 mL round bottom flask, followed by addition of potassium carbonate (4.85 g, 29.4 mmol, 1.1 equiv.), ethanol/water mixture (9:1, 53.4 mL, 0.5 M), and a stir bar. The reaction was stirred at 95 °C for 16 h. The solvent was removed *in vacuo*. The reaction was neutralized with 1N HCl and then the product was extracted with 100 ml dichloromethane and washed sequentially with 1N HCl once, brine solution twice, and dried over magnesium sulfate. The solvent was removed *in vacuo* to provide the final product in green-yellow powder (4.86 g, 20.9 mmol, 78% yield). <sup>1</sup>H NMR (500 MHz, DMSO-*d*<sub>6</sub>) δ 9.58 (s, 1H), 7.50 (dd, *J* = 8.6, 2.1 Hz, 1H), 7.37 (d, *J* = 2.0 Hz, 1H), 6.69 (d, *J* = 8.7 Hz, 1H), 3.61 (t, *J* = 7.2 Hz, 2H), 3.37 (t, *J* = 5.7 Hz, 2H), 2.69 (d, *J* = 6.3 Hz, 2H), 2.52 (t, *J* = 7.2 Hz, 2H), 1.87 – 1.78 (m, 2H); <sup>13</sup>C NMR (126 MHz, DMSO-*d*<sub>6</sub>) δ 189.94, 173.46, 150.04, 131.10, 130.39, 124.83, 122.18, 109.87, 49.41, 47.02, 31.41, 27.72, 21.42; TOF-HRMS (ES+) *m/z* (M+1) calculated for 234.1125, found: 234.1130.

### **(E)-3-(6-(3-(tert-butoxy)-2-cyano-3-oxoprop-1-en-1-yl)-3,4-dihydroquinolin-1(2H)-yl)propanoic acid (3)**

To a 250 mL round bottle flask was added **2** (3.47 g, 14.9 mmol), *tert*-butyl cyanoacetate (10.64 mL, 74.5 mmol, 5 equiv.), pyridine (30 mL, 0.5 M), piperidine (1 mL), and a stir bar. The reaction was stirred at 90 °C for 16 h. The reaction was extracted with 100 mL ethyl acetate and washed sequentially with 1N HCl twice, brine solution twice and dried over magnesium sulfate. The solvent was removed *in vacuo*. The resulting product was purified using column chromatography (7:3 EtOAc/Hexane) to provide a yellow solid (4.2g, 11.9 mmol, 80% yield). <sup>1</sup>H NMR (500 MHz, Acetone-*d*<sub>6</sub>) δ 7.93 (s, 1H), 7.82 (dd, *J* = 8.9, 2.3 Hz, 1H), 7.66 (d, 1H), 6.79 (d, *J* = 8.9 Hz, 1H), 3.75 (t, *J* = 7.1 Hz, 2H), 3.52 (t, 2H), 2.75 (t, *J* = 6.3 Hz, 2H), 2.68 (t, *J* = 7.1 Hz, 2H), 1.94 (p, 2H), 1.54 (s, 9H); <sup>13</sup>C NMR (126 MHz, Acetone) δ 173.15, 163.62, 154.01, 150.29, 133.46, 133.23, 123.35, 119.97, 118.17, 111.14, 95.54, 82.45, 50.39, 47.62, 31.62, 28.46, 28.22, 22.11; TOF-HRMS (ES+) *m/z* (M+1) calculated for 357.1809, found: 357.1812.

### **(E)-N<sub>6</sub>-(3-(6-(2-carboxy-2-cyanovinyl)-3,4-dihydroquinolin-1(2H)-yl)propanoyl)-D-lysine (Rf420DL)**

To a 25 mL round bottom flask was added **3** (143 mg, 0.4 mmol), TSTU (121 mg, 0.4 mmol, 1 equiv.), anhydrous DMF (4 mL, 0.1 M), and diisopropylethylamine (0.2 mL, 1.2 mmol, 3 equiv.) under argon. The reaction was stirred at room temperature for 2 h. Boc-D-Lys-OH (197 mg, 0.8 mmol, 2 equiv.) was added in one portion and the reaction was allowed to continue stirring overnight. The reaction was diluted with 100 mL ethyl acetate and washed sequentially with 1 N HCl once, H<sub>2</sub>O twice, and brine once. The organic layer was dried over anhydrous magnesium sulfate, filtered, and the solvent was removed *in vacuo*. The crude material was dissolved in TFA/DCM (1:1, 3 mL) and stirred at room temperature for 1 h. The solvent was removed *in vacuo*. The product was purified via reverse phase HPLC (10-90% MeCN/H<sub>2</sub>O (v/v) over 10 min, 0.1% TFA (v/v), rt = 7 min) to yield **Rf420DL·TFA salt** (150mg, 0.35 mmol, 87% yield). <sup>1</sup>H NMR (500 MHz, Methanol-*d*<sub>4</sub>) δ 7.96 (s, 1H), 7.74 (dd, *J* = 8.9, 2.3 Hz, 1H), 7.60 (d, *J* = 2.2 Hz, 1H), 6.75 (d, *J* = 8.9 Hz, 1H), 3.90 (dd, *J* = 6.8, 5.9 Hz, 1H), 3.72 (t, *J* = 6.9 Hz, 2H), 3.45 (dd, *J* = 6.6, 4.8 Hz, 2H), 3.17 (t, 2H), 2.74 (t, *J* = 6.3 Hz, 2H), 2.50 (t, *J* = 6.9 Hz, 2H), 1.98 – 1.80 (m, 4H), 1.56 – 1.37 (m, 4H); <sup>13</sup>C NMR (126 MHz, CD<sub>3</sub>OD) δ 173.80, 171.97, 167.22, 155.66, 151.04, 133.89, 133.83, 123.84, 120.42, 119.02, 111.53, 93.85, 53.94, 50.82, 40.00, 34.48, 31.18, 29.84, 28.85, 28.75, 23.35, 22.51; TOF-HRMS (ES+) *m/z* (M+1) calculated for 429.2132, found: 429.2138.

### **methyl 3-(6-iodo-3,4-dihydroquinolin-1(2H)-yl)propanoate (4)**

The following procedure was adapted from previously published literature.<sup>2</sup> To a solution of **1** (16.5 g, 75 mmol) in dioxane:pyridine (1:1, 150 mL) at 0 °C was added molecular iodine (57.1 g, 225 mmol). After 30 minutes, the ice bath was removed and the mixture was allowed to reach room temperature after 1 hour. TLC and mass spec indicated reaction completion and so the reaction mixture was quenched by the addition of saturated Na<sub>2</sub>S<sub>2</sub>O<sub>3</sub> solution (200 mL) and then concentrated under reduced pressure. The aqueous remainder was then extracted with CH<sub>2</sub>Cl<sub>2</sub> (2 x 200 mL). The combined organic layer was washed with water (100 mL) and brine (100 mL) then dried over MgSO<sub>4</sub> and concentrated *in vacuo* to provide a burgundy oil (19.2 g, 55.6 mmol, 74% yield) which was used directly in the next reaction. <sup>1</sup>H NMR (400 MHz, Chloroform-*d*) δ 7.28 (dd, *J* = 8.7, 2.2 Hz, 1H), 7.21 (dt, *J* = 2.1, 1.0 Hz, 1H), 6.35 (d, *J* = 8.7 Hz, 1H), 3.68 (s, 3H), 3.58 (dd, *J* = 8.0, 6.5 Hz, 2H), 3.27 (t, 2H), 2.69 (t, *J* = 6.4 Hz, 2H), 2.57 (t, 2H), 1.90 (p, 2H); ESI MS *m/z* (M+H) found 346.0

### **Potassium trifluoro(5-formylthiophen-2-yl)borate**

5-formyl-2-thienylboronic acids (7.6 g, 49 mmol) was dispersed in MeOH:H<sub>2</sub>O solution (4:1, 250 mL) then KHF<sub>2</sub> (11.5 g, 147 mmol) was added. The reaction mixture was stirred for 12 hours at room temperature then concentrated *in vacuo* to provide a grey solid which was carried on directly to the next reaction.

### **3-(6-(5-Formylthiophen-2-yl)-3,4-dihydroquinolin-1(2H)-yl)propanoic acid (5)**

The following procedure was adapted from previously published literature.<sup>2</sup> To a solution of **4** (15.2 g, 44 mmol) in THF:MeOH:H<sub>2</sub>O solution (2:2:1, 375 mL) at 0 °C was added LiOH·H<sub>2</sub>O (2 g, 48 mmol). The reaction mixture was closely monitored by TLC, and upon consumption of starting material was immediately quenched by the addition of 0.5 M HCl (100 mL) and the reaction solvents were removed *in vacuo*. The residue was re-constituted with EtOAc (200 mL) and the organic extract was washed with water (100 mL) and brine (100 mL) then dried over MgSO<sub>4</sub>. The organic solution was concentrated *in vacuo* to a beige solid (13.5 g, 40 mmol, 92% yield) which was submitted directly to the next reaction. ESI MS *m/z* (M+H) found 332.0. To the potassium organotrifluoroborate salt was added the beige solid intermediate (13.5 g, 40 mmol) and EtOH (200 mL), followed by Cs<sub>2</sub>CO<sub>3</sub> (31.8 mL, 98 mmol) and Pd(OAc)<sub>2</sub> (90 mg, 0.4 mmol). The reaction mixture was heated to reflux (120 °C) until the starting material was consumed, as indicated by TLC. The reaction mixture was concentrated *in vacuo*, diluted with CH<sub>2</sub>Cl<sub>2</sub> (300 mL), and then *slowly* quenched by the addition of 8 M HCl (150 mL). The organic layer was washed with water (200 mL), brine (200 mL), then dried over MgSO<sub>4</sub> and concentrated under reduced pressure. The residue was purified by flash column chromatography to provide an orange solid (7.58 g, 24 mmol, 60 % yield). <sup>1</sup>H NMR (400 MHz, Chloroform-*d*) δ 9.81 (s, 1H), 7.66 (d, *J* = 4.0 Hz, 1H), 7.39 (d, *J* = 8.9 Hz, 1H), 7.28 (s, 1H), 7.21 (d, *J* = 4.0 Hz, 1H), 6.61 (d, *J* = 8.6 Hz, 1H), 4.15 (q, *J* = 7.1 Hz, 2H), 3.66 (t, *J* = 7.2 Hz, 2H), 3.36 (t, *J* = 5.6 Hz, 2H), 2.78 (t, *J* = 6.4 Hz, 2H), 2.61 (t, *J* = 7.1 Hz, 2H), 1.96 (p, *J* = 6.0 Hz, 2H), 1.27 (t, 3H); <sup>13</sup>C NMR (126 MHz, DMSO) δ 183.03, 173.18, 154.91, 145.82, 139.69, 139.04, 126.80, 125.52, 122.49, 121.80, 119.40,

110.43, 48.71, 46.47, 30.92, 27.35, 21.31.  $R_f = 0.4$  [Hexane:{EtOAc:EtOH(3:1)2% AcOH}(2:1)]; TOF-HRMS (ES+)  $m/z$  (M+1) calculated for 316.0963, found: 316.1005.

**(E)-3-(6-(5-(3-(tert-butoxy)-2-cyano-3-oxoprop-1-en-1-yl)thiophen-2-yl)-3,4-dihydroquinolin-1(2H)-yl)propanoic acid (6)**

The thiophene aldehyde derivative (3.5 g, 11.1 mmol, **5**) was dissolved in pyridine (55 mL). To this dark solution was added *tert*-butyl 2-cyanoacetate (8 mL, 55.5 mmol) and piperidine (5 mL). Upon addition of the piperidine, the solution turned dark, cherry red. The mixture was then heated to 90 °C for 18 hours. HPLC and TLC indicated full consumption of starting material and so the solution was concentrated under reduced pressure and solvents were removed azeotropically with toluene. The residue was dissolved in EtOAc (200 mL), then washed with 1 M HCl (100 mL), water (100 mL), brine (100 mL), then dried over Na<sub>2</sub>SO<sub>4</sub> then concentrated *in vacuo* to provide dark red/black highly viscous oil which solidified to a glass upon standing. The material was sufficiently pure to be carried on to the next reaction (4.2 g, 9.66 mmol, 87% yield). An analytical sample was prepared by preparative HPLC. <sup>1</sup>H NMR (400 MHz, Chloroform-*d*) δ 8.16 (s, 1H), 7.63 (d,  $J = 4.1$  Hz, 1H), 7.43 (dd,  $J = 8.6, 2.3$  Hz, 1H), 7.31 (d,  $J = 2.3$  Hz, 1H), 7.21 (d,  $J = 4.1$  Hz, 1H), 6.61 (d,  $J = 8.7$  Hz, 1H), 3.69 (t,  $J = 7.1$  Hz, 2H), 3.38 (t,  $J = 5.7$  Hz, 2H), 2.80 (t,  $J = 6.3$  Hz, 2H), 2.69 (t,  $J = 7.1$  Hz, 2H), 1.99 (p,  $J = 11.9, 6.1$  Hz, 2H), 1.57 (s, H); <sup>13</sup>C NMR (126 MHz, CDCl<sub>3</sub>) δ 177.05, 162.59, 156.18, 146.06, 145.73, 139.71, 132.91, 127.69, 125.93, 123.49, 121.82, 121.18, 116.89, 110.96, 97.36, 83.23, 49.70, 47.13, 31.25, 28.17, 27.96, 21.82; TOF-HRMS (ES+)  $m/z$  (M+1) calculated for 439.1692, found: 439.1709

**(E)-N<sub>6</sub>-(3-(6-(5-(2-carboxy-2-cyanovinyl)thiophen-2-yl)-3,4-dihydroquinolin-1(2H)-yl)propanoyl)-D-lysine (Rf470DL)**

A solution of **6** (220 mg, 0.5 mmol) in DMF (5 mL) was purged with Argon gas. After 15 minutes, TSTU (151 mg, 0.5 mmol) and DIPEA (0.25 ml, 1.5 mmol) were added, and the mixture was stirred for 2 hours at room temperature. Progress of the TSTU activation was monitored by HPLC and mass spectrometry. Once starting material was fully consumed, Boc-D-lysine (123 mg, 0.5 mmol) was added at once, and the mixture was stirred at room temperature for 20 hours. The reaction mixture was diluted with EtOAc (50 mL) and 1 M HCl (50 mL), followed by extraction with EtOAc (2 x 50 mL), wash with brine (50 mL), dried over MgSO<sub>4</sub> and then concentrated *in vacuo*. The crude residue was diluted with CH<sub>2</sub>Cl<sub>2</sub> (3 mL) and TFA (3 mL). The solution was stirred at room temperature for 2 hours and then concentrated to a red residue which was purified by preparative HPLC (10-90% MeCN/H<sub>2</sub>O over 10 min,  $r_t = 8$  min). The fractions containing the product were lyophilized to provide **Rf470DL·TFA salt** (272 mg, 43.5 mmol, 87% yield). <sup>1</sup>H NMR (500 MHz, DMSO-*d*<sub>6</sub>) δ 8.35 (d,  $J = 1.9$  Hz, 1H), 7.89 (dd,  $J = 4.2, 2.0$  Hz, 1H), 7.82 (t,  $J = 5.6$  Hz, 1H), 7.46 – 7.44 (m, 1H), 7.42 (d, 1H), 7.31 (d,  $J = 2.6$  Hz, 1H), 6.69 (d,  $J = 8.7$  Hz, 1H), 3.83 (t,  $J = 6.4$  Hz, 1H), 3.57 (t,  $J = 7.1$  Hz, 2H), 3.32 (t,  $J = 5.6$  Hz, 2H), 3.06 (q,  $J = 6.4$  Hz, 2H), 2.73 (t,  $J = 6.4$  Hz, 2H), 2.37 (t,  $J = 7.0$  Hz, 2H), 1.91 – 1.71 (m, 4H), 1.39 (ddd,  $J = 35.7, 10.4, 6.3$  Hz, 4H); <sup>13</sup>C NMR (126 MHz, DMSO) δ 171.06, 170.41, 164.13, 155.71, 146.53, 146.23, 142.33, 131.61, 126.82, 125.71, 122.53, 121.88, 119.11, 117.01, 110.60, 95.21, 51.93, 48.80, 47.27, 38.19, 32.58, 29.70, 28.57, 27.37, 21.79, 21.29; TOF-HRMS (ES+)  $m/z$  (M+1) calculated for 511.2015, found: 511.1991

**(E)-2-cyano-3-(5-(1-(3-methoxy-3-oxopropyl)-1,2,3,4-tetrahydroquinolin-6-yl)thiophen-2-yl)acrylic acid (7)**

To a 10 ml round bottle flask, **6** (29.1 mg, 0.066 mmol), K<sub>2</sub>CO<sub>3</sub> (45.6 mg, 0.33 mmol), and DMF (1.32 ml) were added. After stirring for 20 min, methyl iodide (4.1 μl, 0.066 mmol) was added to the reaction and the reaction was stirred at 40 °C for 24 hours. The desired compound was purified using column chromatography (5% MeOH in CHCl<sub>3</sub>, v/v). The solvent was then removed *in vacuo* to give deep red powder (20.9 mg, 0.046 mmol, 70 % yield). The purified material was dissolved in DCM/TFA mixture in 2:1 ratio and stirred for 1 hour at room temperature. The solvent was then removed *in vacuo* and the compound was purified using HPLC (50-90% MeCN/H<sub>2</sub>O over 10 min, 0.1% TFA,  $r_t = 8.5$  min.) The solvent was removed *in vacuo* (17.3 mg, 0.044 mmol, 95% yield). <sup>1</sup>H NMR (500 MHz, DMSO-*d*<sub>6</sub>) δ 8.36 (s, 1H), 7.90 (d,  $J = 4.1$  Hz, 1H), 7.47 (d,  $J = 4.1$  Hz, 1H), 7.44 (dd,  $J = 8.6, 2.3$  Hz, 1H), 7.32 (d,  $J = 2.6$  Hz, 1H), 6.68 (d,  $J = 8.7$  Hz, 1H), 3.63 (d,  $J = 4.4$  Hz, 2H), 3.62 (s, 3H), 3.33 (t,  $J = 5.7$  Hz, 2H), 2.74 (t,  $J = 6.3$  Hz, 2H), 2.61 (t,  $J = 7.0$  Hz, 2H), 1.87 (p,  $J = 6.3$  Hz, 2H); <sup>13</sup>C NMR (126 MHz, DMSO-*d*<sub>6</sub>) δ 171.66, 163.65, 155.19, 145.98, 145.85, 141.30, 131.56, 126.59,

125.40 , 122.58 , 121.78 , 119.30 , 116.53 , 110.41 , 51.07 , 48.53 , 46.25 , 30.70 , 27.08 , 21.09 . TOF-HRMS (ES+)  $m/z$  (M+1) calculated for 453.1848, found: 453.1847.

**(E)-N<sub>6</sub>-(3-(5-(1-(2-carboxyethyl)-1,2,3,4-tetrahydroquinolin-6-yl)thiophen-2-yl)-2-cyanoacryloyl)-L-lysine (Rf490DL)**

The cyano-acrylate ethyl ester derivative (17.3 mg, 0.044 mmol, 7) was dissolved in 1 mL DMF and purged with Argon gas. After 15 minutes, TSTU (27 mg, 0.088 mmol) and DIPEA (0.024 ml, 0.132 mmol) were added and the reaction was stirred for 2.5 hours at room temperature. TSTU activation was monitored by HPLC and mass spectrometry. After starting material was completely consumed, Boc-D-lysine (22.2 mg, 0.088 mmol) was added to the reaction. This was stirred overnight at room temperature. The solution was then diluted with EtOAc (15 mL), followed by washing with 1M HCl (10 mL) twice, brine (10 mL) once, dried over MgSO<sub>4</sub> and then concentrated *in vacuo*. The crude residue was dissolved in DCM/TFA mixture in 2:1 ratio and stirred for 2 hours at room temperature. After removing the solvent *in vacuo*, the resulting free acid derivative was dissolved in THF/H<sub>2</sub>O mixture (1:1, 2 ml for each). Once the starting material was fully dissolved, LiOH was added (5.3 mg, 0.22 mmol). This reaction was stirred for 1 hour at 40 °C, followed by neutralization using 1M HCl. After removing the solvent *in vacuo*, the crude product was purified by preparative HPLC (10-90% MeCN/H<sub>2</sub>O over 10 min, rt= 8 min). The fractions containing the product were lyophilized to provide **Rf490DL·TFA salt** (5.5 mg, 0.009 mmol, 20% yield). <sup>1</sup>H NMR (500 MHz, DMSO-*d*<sub>6</sub>) δ 8.22 (s, 1H), 8.05 (t, *J* = 5.6 Hz, 1H), 7.76 (d, *J* = 4.1 Hz, 1H), 7.40 (dd, *J* = 8.9, 2.9 Hz, 2H), 7.28 (d, *J* = 2.2 Hz, 1H), 6.66 (d, *J* = 8.7 Hz, 1H), 3.85 (t, *J* = 6.3 Hz, 1H), 3.58 (t, *J* = 7.1 Hz, 2H), 3.33 (t, *J* = 5.7 Hz, 2H), 3.22 (q, *J* = 6.6 Hz, 2H), 2.72 (t, *J* = 6.3 Hz, 2H), 2.50 (t, *J* = 6.5 Hz, 2H), 1.90 – 1.70 (m, 4H), 1.62 – 1.30 (m, 4H); <sup>13</sup>C NMR (126 MHz, DMSO-*d*<sub>6</sub>) δ 172.67 , 170.52 , 161.04 , 153.49 , 145.73 , 142.60 , 139.44 , 131.84 , 126.43 , 125.22 , 122.54 , 121.49 , 119.37 , 116.86 , 110.43 , 98.65 , 51.86 , 48.52 , 46.37 , 39.07 , 31.00 , 29.51 , 28.19 , 27.14 , 21.58 , 21.17. TOF-HRMS (ES+)  $m/z$  (M+1) Calculated for 511.2015, found: 511.2011

**SI-Methods of data acquisition**

**Culture growth.** Strain characteristics and growth conditions are shown in Supplementary Table 1. Bacterial cells were inoculated from -80°C frozen tubes onto LB agar plates and incubated overnight at 37 °C for *Bacillus subtilis* and *Escherichia coli*, or 30°C for *Streptomyces venezuelae*. Cells from single colonies were transferred to liquid LB medium and incubated in an Innova® 44R shaker at 37 °C or 30 °C. After the cell cultures reached OD<sub>600</sub>~0.5, they were diluted with LB medium to OD<sub>600</sub>~0.05 (10x) and again incubated in the shaker until OD<sub>600</sub>~0.5. The cells were then used for labeling experiments.

**Rotor/standard Fluorescent D-amino acid labeling.** RfDAA/FDAA stock solutions were prepared in DMSO at a concentration of 100 mM and stored at -20°C before use. For long-pulse labeling of *B. subtilis* and *E. coli*, exponential phase cultures were diluted with fresh LB broth containing 1 mM RfDAA/FDAA to OD<sub>600</sub>~0.05 and incubated for 1h. The cells were then imaged immediately using a Nikon Ti-E inverted microscopy system without washing and fixation. For short-pulse labeling of *S. venezuelae*, RfDAA/FDAA stock solution was added directly to exponential phase cultures to a final concentration of 0.5 mM, followed by incubating at 30 °C with shaking for 15 min. The cells were then imaged immediately. For washed samples, FDAA-labeled cells were collected by centrifugation (7000 g, 1 min) and then resuspended in 37 °C fresh LB broth. This process was repeated twice and the washed cells were resuspended in LB broth before imaging. For time-lapse experiments with unwashed cells, exponentially growing cells were directly used for imaging.

**Image sample preparation.** For endpoint imaging, 24X50 mm coverslips (#1.5) were used as sample supports for the inverted microscope system. The coverslips were rinsed with ethanol and water twice, and air-dried before use. Bacterial cells were added to the coverslips and an 8x8-mm wide, 2-mm thick PBS-agarose pad (SeaKem LE Agarose) was laid on top of the cells. The coverslip-pad combination was placed onto a customized slide holder on the microscope

with the pad facing upwards. For time-lapse imaging, RfDAAs (100 mM stock solution in DMSO) was dissolved in molten LB-agarose (1.5 %, w/v). The mixture was then added to cavity slides (75x25 mm, 15 mm cavity diameter, GEM Industrial Corporation), and a 22x22 mm coverslip was laid on top to flatten the mixture. The mixture was allowed to solidify for 2 h before use. The coverslip was then removed and bacterial cells were added to the top of the pad, followed by laying a new 22x22 mm coverslip on top and sealing it with VLAP (mixture of Vaseline, Paraffin and Lanolin, 1:1:1). The cells were then imaged at optimal growth temperature.

**Image acquisition and data processing.** Phase contrast and fluorescence images were acquired using a Nikon Ti-E inverted microscope equipped with a 1.4NA Plan Apo 60X oil objective and Andor iXon EMCCD camera. An objective warmer (Warner Instrument Corporation, USA) was used to maintain the sample temperature for time-lapse experiments. NIS-Element AR (Version 5.02) was used for image acquisition. Exposure, light source power, EM gain and time-lapse interval were optimized individually for each sample/experiment. Filter selection: for **Rf420DL**: Ex 395/25 nm (DAPI), Em 510/40 nm (FITC); for **Rf470DL** and **Rf490DL**: Ex 470/24 nm (FITC), Em 595/40 nm (Cy3). Image processing was performed in FIJI (Version 1.51). Images were scaled without interpolation, cropped and rotated. Linear adjustment was performed to optimize contrast and brightness of the images. Quantitative measurement of FDAA labeling intensity was achieved using a FIJI plugin, MicrobeJ<sup>3</sup>, where cells were identified in the phase contrast channel with width limit from 0.3 to 2  $\mu\text{m}$  and length above 1  $\mu\text{m}$ . FDAA labeling intensity was then quantified and averaged ( $N > 50$ ). For figures 2, 3, Supplementary 2, Supplementary 3, Supplementary 4, and Supplementary 7, cells that can nicely represent the whole population were chosen and shown. GraphPad Prism 7 was used for statistical calculation (mean, standard deviation, the linear regression) and data plotting.

**Fluorescence spectra and intensity acquisition.** Spectra wavelength, absorbance, and fluorescence intensity of RfDAAs were determined using a SpectraMax M2 plate reader (Molecular Devices, USA). 48/96-well plates (Falcon<sup>®</sup> Polystyrene, black walls with clear bottom) or cuvettes (1 cm width, methacrylate) were used for the measurements.

For spectra measurement, RfDAA (100 mM stock solution, DMSO) was diluted with 1:1 mixture of 1X PBS (NaCl 8 g/L, KCl 0.2 g/L,  $\text{Na}_2\text{HPO}_4 \cdot 2\text{H}_2\text{O}$  1.78 g/L,  $\text{KH}_2\text{PO}_4$  0.27 g/L, pH 7.4) and glycerol to a final concentration of 0.01 mM. Excitation (Ex) spectrum was determined by recording the absorbance with excitation light ranged from 350 to 850 nm (1 nm increment) using cuvettes (polymethyl methacrylate). The wavelength at  $\sim 20$  nm below the maximum absorbance was used as the excitation wavelength for measuring emission (Em) spectra. For extinction coefficient measurement, series dilutions of RfDAA were made in 1X PBS (0.04, 0.02, 0.01, and 0.005 mM). The absorbance of each sample at the maximum Ex wavelength was record. Extinction coefficient was then determined by fitting the data to Beer's law.

**Bacteria growth curves.** *B. subtilis* WT and *E. coli imp* cultures were grown to exponential phase and were diluted with fresh LB medium containing 1 mM RfDAAs to  $\text{OD}_{600} \sim 0.05$ . The diluted cultures were transferred to a 48-well microplate (0.5 ml for each well). The growth curves were obtained by measuring the absorbance at 600 nm in time-lapse for 12 hours using the SpectraMax M2 plate reader (37°C, 3 min interval, with shaking between each measurement).

**Measurement of distribution coefficient ( $\text{LogD}_{7.4}$ ).** RfDAAs (100 mM stock solution in DMSO) were diluted with 2 mL 1X PBS to a final concentration of 0.05 mM. After measuring the absorbance at the maximum Ex wavelength (SpectraMax M2 plate reader with cuvettes), the RfDAA-PBS solution was extracted with 2 mL 1-octanol once. The absorbance of the PBS layer was measured again to calculate the amount of remaining RfDAA. The  $\text{LogD}_{7.4}$  value was calculated with the following equation (modified from Lombardo *et al*).<sup>4</sup>

$$\text{LogD}_{\text{PBS},\text{pH}7.4} = \text{Log} \frac{[\text{Solute}]_{1\text{-octanol}}}{[\text{Solute}]_{\text{PBS},\text{pH}7.4}}$$

**Measurement of viscosity sensitivity.** RfDAAs (100 mM stock solution in DMSO) were diluted in PBS-glycerol solution (1x PBS containing 0%, 20%, 40%, 60% or 80% glycerol, v/v, pH 7.4) to a final concentration of 0.1 mM. Their fluorescence intensity was measured at the maximum Em wavelength with excitation at the maximum Ex wavelength (96-well microplate). The viscosity sensitivity was calculated using the following equation, where  $\eta$  is dynamic viscosity of the solvents,  $I$  is the emission intensity of the FDAAs,  $c$  is a constant depending on the temperature, and  $x$  is the viscosity sensitivity of the dye.<sup>5</sup> The dynamic viscosity of PBS-glycerol solution was calculated based on the work by Cheng *et al.* with the assumption that PBS viscosity equals to water viscosity.<sup>6</sup>

$$\text{Log}I = x \log \eta + c$$

For RfDAA-labeled *B. subtilis*, long-pulse labeled cells were first prepared as described above. The cells were washed and then fixed with ice-cold ethanol (70%, v/v) for 1 h. The fixed cells were washed with 1x PBS twice and resuspended in PBS-glycerol solution (1x PBS containing 0%, 20%, 40%, 60% and 80% glycerol, v/v, pH 7.4). The viscosity sensitivity was measured and calculated as described above.

**Measurement of quantum yield.** Fluorescein was used as standard for the measurements.<sup>7</sup> RfDAAs and fluorescein were dissolved in 1X PBS containing 50% (v/v) glycerol and 2.5% DMSO (v/v) to prepare working solutions ranging from 10  $\mu\text{M}$  to 50  $\mu\text{M}$ . The absorbance of each sample at 460 nm was recorded. Next, the fluorescence spectrum of each sample was measured with excitation at 460 nm (fluorescein: 475-725 nm, **Rf420DL**: 475-725 nm, **Rf470DL** : 500-850 nm, **Rf490DL**: 500-850 nm). The slope of integrated fluorescence intensity over absorbance was then calculated. Integrated fluorescence intensity was calculated using Prism (Area under Curve). The quantum yield was calculated using the following equation:

$$\Phi_{dye} = \Phi_{ST} \left( \frac{\text{Slop}_{dye}}{\text{Slop}_{ST}} \right)$$

, where  $\phi$  is quantum yield. The parameter of refractive index of the solvent is not shown in the equation because the same solvent was used for all the samples. All the measurements were performed at 25 °C. The increment of spectrum measurement was 2 nm.

**Measurement of thermostability.** RfDAAs (100 mM stock solution, DMSO) were diluted with 1X PBS or LB to a final concentration of 0.05 mM. The absorbance at the maximum Ex wavelength was measured (SpectraMax M2 plate reader, cuvettes used). The solutions were then incubated at RT, 37 °C or 60 °C without light exposure for up to 24 h. The thermostability of FDAAs was calculated as the ratio of final absorbance to the initial absorbance of FDAA:

$$\text{Thermostability} = \frac{A_{\text{final}}}{A_{\text{initial}}} \times 100\%$$

**Sacculi purification.** The purification protocol was modified from Kuru *et al.*<sup>8</sup> 50 mL cell cultures labeled with RfDAA (long-pulse labeling) were prepared as described above. The cells were collected by centrifugation, washed once with 1x PBS and fixed with ice-cold ethanol (70%, v/v) for 1 h. The fixed cells were collected, followed by washing with 1x PBS (pH 7.4) twice and 1x PBS-SDS solution (0.5% SDS, w/v, pH 7.8) once. The cells were then incubated in the 1x PBS-SDS solution containing 1.5 mg/ml pronase E (Sigma-Aldrich, *Streptomyces griseus*) for 2 hours at 60 °C. After the cells were collected, they were washed with H<sub>2</sub>O once, resuspended in 4% SDS-H<sub>2</sub>O solution (w/v) and boiled for 1 hour. The boiled pellets were washed with H<sub>2</sub>O twice and then imaged.

**Transpeptidase activity assays and antibiotic tests.** For end-point measurements, **Rf470DL** stock solution (100 mM in DMSO) and acetyl-tripeptide substrate ( $N_{\alpha}$ ,  $N_{\epsilon}$ -Diacetyl-L-Lys-D-Ala-D-Ala, Bachem, 100 mM in water) were diluted

with Kahne buffer (62.5 mM HEPES, pH 7.5, 10 mM MnCl<sub>2</sub>, 1.25 mM Tween-20) to a final concentration of 1 mM and 10 mM, respectively. The reaction was initiated by the addition of *S. aureus* PBP4 (final concentration: 0.4 mg/ml), which was prepared following reported procedures by Yuan Qiao *et al.*<sup>9</sup> The mixture was incubated at 37 °C for 1 h with continuous shaking. The fluorescence intensity at 640 nm was then measured using the SpectraMax M2 plate reader with excitation at 470 nm. For real-time measurements, the reaction mixtures were transferred to a 96-well plate and directly incubated in the plate reader. The temperature control and shaking function were turned on. Fluorescence was recorded every 5 minutes with shaking for a total of 1 h. After the reaction, the mixtures were analyzed by reverse-phase HPLC (10-90% MeCN/H<sub>2</sub>O over 10 min, 0.1% TFA). Absorbance at 470 nm and ELSD (evaporative light scattering detector) were used for the signal monitoring. For antibiotic treatments, 1 mM (0.1 equiv. to the substrate) of antibiotic was incubated with the enzyme for 15 minutes prior to enzyme addition.

Similar protocols were used for LdtA and Sortase A assays. For the LdtA assay, synthetic acetyl-tetrapeptide (Diacetyl-L-Ala-D-iGlu-L-Lys-D-Ala, acylation on N<sub>α</sub>-L-Ala and N<sub>ε</sub>-L-Lys) was used as the substrate. LdtA was obtained from Felipe Cava, Umea University. LdtA (15 μM) and the substrate (0.5 mM) were added to Tris buffer (Tris 50mM, NaCl 150 mM, pH 7.5) containing 1 mM **Rf470DL**. The reaction was carried out at 37 °C for 1 h with 1 min reading interval. For the Sortase assay, synthetic acetyl-pentapeptide (acetyl-L-Leu-L-Pro-L-Glu-L-Thr-Gly, acylation on N<sub>α</sub>-Leu) was used as the substrate. Sortase A plasmid was purchased from Addgene (Cat. 21931). SrtA (2 μM) and the substrates (10 mM) were added to Tris-Ca<sup>2+</sup> buffer (Tris 50mM, NaCl 150 mM, 5mM CaCl<sub>2</sub>, pH 7.5). The reaction was carried out at 37 °C for 4 h with 10 min reading interval.

**β-lactamase activity assays of PBP4.** β-lactamase assays to determine the relative enzymatic activity of PBP4 were conducted as follows.<sup>10</sup> Each antibiotic (Sigma, Ampicillin: A9518, Carbenicillin: C9231, Cefoxitin: C4786, Penicillin G: 13752; MP Biomedicals, Piperacillin: 156268) was pre-incubated with the enzyme for 30min before adding Nitrocefin (Cayman chemical, 15424) to initiate the enzyme reaction. The final concentration for each antibiotic was 20mM while that for Nitrocefin was 1mM. Antibiotic stocks were prepared in ultrapure water while the Nitrocefin stock was prepared in DMSO. Each assay contained a final concentration of 0.1mg/ml BSA (Sigma, item P0834) and 5% glycerol (v/v). We found that the BSA and glycerol helped with the solubility of Nitrocefin and lead to a consistent absorbance reading by the spectrophotometer. The assays were incubated for 10 min at room temperature in a 96-well plate before reading the absorbance at 486nm. Each experiment was conducted in duplicate with two technical replicates.

## **SI-Discussions**

### **Supplementary discussion 1. Photochemical and physical properties of RfDAAs**

RfDAAs have a relatively large Stoke shift compared to most commonly used fluorophores. One might have to customize their microscope settings for imaging these probes. For **Rf420DL**, a purple light source (e.g. 395nm light for DAPI dye) can be used for excitation and a green emission filter (e.g. 510/40 nm for GFP) can be used for signal detection. **Rf470DL** and **Rf490DL** are ideally excited by a blue light source (e.g. 470 nm light for GFP) and imaged using an orange emission filter (e.g. 595/40 for Cy3). Because of its broad bandwidth of spectra, **Rf490DL** signal can also be excited by using a green light source (i.e. 510/25 for YFP), which could further reduce photo-toxicity on cells. We evaluated the brightness of RfDAAs by measuring their quantum yield ( $\phi$ ) and molar absorptivity ( $\epsilon$ ). The measured  $\phi$  value of RfDAAs ranges from 0.01 to 0.04 in 50% glycerol-PBS (Table 1). We note that the fluorescence intensity of RfDAAs is dependent upon solvent viscosity. The calculated absorptivity of RfDAAs ranges from ~20,000 to ~30,000 M<sup>-1</sup>cm<sup>-1</sup>. Of all the probes, **Rf470DL** has the highest quantum yield and absorptivity, and thus is predicted to possess the highest brightness. On the other hand, the relative low  $\phi$  and  $\epsilon$  value of **Rf420DL** might contribute to its low signal intensity in *E. coli* labeling experiments, as mentioned in the main text.

Water-solubility plays an important role in PG labeling because it determines the maximum working concentration of the dyes in culture solution as well as the level of non-specific binding to cell membranes.<sup>11</sup> High water-solubility, which



gives low membrane binding affinity, is usually preferred. The distribution coefficient ( $\text{LogD}_{7.4}$ ) of RfDAAs were measured and they all showed high water solubility comparable to HADA (Table 1).<sup>12,13</sup> We also determined the thermostability of RfDAAs to ensure their resistance to culturing temperature during labeling process. We incubated RfDAA solutions (in PBS) at 60 °C for 24 hours and measured the retention of absorbance signal. A retention higher than 95% compared to the initial point was found for all RfDAAs.

### Supplementary discussion 2. Comparison between Rf470DL and Rf490DL

**Rf470DL** and its structural isomer, **Rf490DL**, show consistent labeling pattern in *B. subtilis*, *E. coli* and *S. venezuelae*. There is also no significant difference in viscosity sensitivity, solubility and bio-compatibility between them. However, coupling D-Lys to the vinyl carboxylate group results in a ~20 nm red-shift in excitation and emission spectra. We attribute the wavelength shift to the change of electronegativity of the electron acceptor moiety of the rotor molecules. Having an amide group at the vinyl position allows electron resonance from the quinoline amine to the amide oxygen. The resonance stabilizes the charge transfer state of the molecule and thus decreases the required energy for inducing charge transfer. Thus, a red-shifted wavelength can excite **Rf490DL**. This result also suggested that the excitation and emission spectra of RfDAAs could be adjusted by changing the functional group of the electron acceptor moiety.

### Supplementary discussion 3. Optimization of RfDAA labeling condition to reduce background fluorescence

Signal-to-background (S/B) ratio is commonly used to evaluate the quality of labeling experiments and dye effectiveness.<sup>11</sup> RfDAAs labeling show relatively low S/B ratio (~2, unwashed condition), mainly resulting from the background fluorescence of free RfDAAs (partially turned-on by the environment). Washing out excess RfDAAs before imaging can effectively reduce background fluorescence but will also restrain time-lapse applications of the probes. Therefore, optimization of RfDAA labeling to enable imaging without washing is required. For in-solution labeling, such as end-point experiments, background fluorescence could be reduced by decreasing the volume of sample solution used in microscopy imaging. Also, with an inverted microscope, one can use agarose pad to cover cell samples instead of using regular coverslips. This leads to lower background signal probably because the agarose absorbs excess RfDAAs from the medium.

In time-lapse experiments shown in Fig. 3, we dissolved RfDAAs in molten LB-agarose and allowed the mixture to solidify in cavity slides. RfDAAs show stronger fluorescence in agarose pads compared to free solution, which leads to higher background signal in our time-lapse experiments. In general, higher agarose percentages in the pad gives stronger RfDAA background fluorescence, suggesting an increased steric hindrance. A range of agarose concentration from 1 to 1.5 % (w/v) is recommended. The thickness of the pad also contributes to background level when epifluorescence microscopy is used. A thin pad usually provides better S/B ratio. One can also use TIRFM (total internal reflection fluorescence microscopy) to reduce the background fluorescence from the pad. Finally, although a higher concentration of probe usually results in better PG labeling intensity, it also leads to higher background signal from the pad. Adjustment of RfDAA concentration for optimizing S/B ratio is required.

Time-lapse experiments using a microfluidic system were tested with *B. subtilis* and **Rf470DL**. The micro-chamber and channels were constructed using polydimethylsiloxane (PDMS). We found that **Rf470DL** showed strong background fluorescence in this system. This is probably caused by the non-specific binding of **Rf470DL** to PDMS, which turns on **Rf470DL** fluorescence.

### Supplementary discussion 4. The outer-membrane permeability of RfDAAs

The outer membrane (OM) of Gram-negative bacteria is an effective physical barrier against chemical entry from the environment. The cells import water-soluble molecules, such as **RfDAAs**, into periplasm through protein transporters, known as porins. It is reported that, in *E. coli*, a molecular weight (MW) of ~600 g/mole is the cutoff limit for the porin-mediated transportation<sup>14</sup>. **RfDAAs** have smaller MW than the cutoff limit, which should enable labeling in *E. coli* WT. However, a poor labeling efficiency of **RfDAAs** was observed in the study. We note that, in addition to molecular weight,

solubility (hydrophobicity), ring content and rotation availability of molecules are also highly related to their OM permeability, as reported by Davis *et al.*<sup>15</sup> These parameters, together, could result in the unexpected low labeling efficiency of **RfDAAs** in *E. coli* WT.

### **Supplementary discussion 5. Sensitivity of RfDAAs to the size of substrate in the *in vitro* transpeptidation assays**

It is unclear how sensitive RfDAAs are to the size of substrate in the transpeptidation assays. In our current setup, we used diacetyl-tripeptides (Lys-D-Ala-D-Ala) as the substrate and observed an ~2-fold increase of signal compared to the control samples. Because RfDAAs are sensitive to the spatial restriction, it is expected that larger substrates can lead to stronger signal change in the assays. To test this, we replaced the tripeptide substrate with PG pentapeptides, L-ala(Acetyl)-D-glu-L-lys(Acetyl)-D-ala-D-ala. We found a slightly improved signal change compared to the use of tripeptides (data not shown). We expected that, with the use of larger PG substrate, such as Lipid II, the signal change of the assay would be more dramatic. Experiments using large PG substrates have not been done due to the limited access of the substrates at this point. In future studies, we will test the transpeptidation assays using various substrates, such as Park's nucleotides and Lipid II.

### **Supplementary discussion 6. Malononitrile derivatives of Rf420DL and Rf470DL**

Malononitrile derivatives are often used for the design of fluorescent molecular rotors (Supplementary Fig. 12a).<sup>16,17</sup> We synthesized the malononitrile derivatives of **Rf420DL** and **Rf470DL**, namely **Rf460DL** and **Rf540DL**, based on the same synthesis strategies except that *t*-butyl cyanoacetate was replaced with malononitrile (Fig. 1). The synthesis was confirmed by HRMS and <sup>1</sup>H NMR (data not shown). We found that **Rf460DL** has a ~40 nm red-shift in excitation; and **Rf540DL** has a ~70 nm red-shift compared to **Rf420DL** and **Rf470DL**, respectively. This desirable red-shift might result from the increased electronegativity of the electron acceptor moiety in the structure, as discussed above. However, **Rf460DL** and **Rf540DL** have low thermo-stability. An incubation at 37 °C in LB broth for 24 hours resulted in more than 90% degradation of these compounds (Supplementary Fig. 12b). This is probably due to the high reactivity of the malononitrile groups. Also, the malononitrile group is much more lipophilic than the cyanoacetate group, which leads to low water-solubility of **Rf460DL** and **Rf540DL**. **Rf540DL** barely dissolves in aqueous solution, such as PBS and culture medium. Indeed, **Rf540** caused strong and non-specific membrane binding. Due to these limitations, **Rf460DL** and **Rf540DL** were not used for bacteria labeling and transpeptidase activity assays.

### **Movie legends**

#### **Supplementary Movie 1.**

Time-lapse microscopy of PG synthesis in *S. venezuelae* using **Rf470DL**. The cells were imaged in a cavity slide filled with LB-agarose (1.5%, w/v) containing 0.5 mM **Rf470DL**. The imaging was carried out at 30 °C for 3 hours. Left: merged channel from phase contrast and fluorescence channels; right: fluorescence channel.

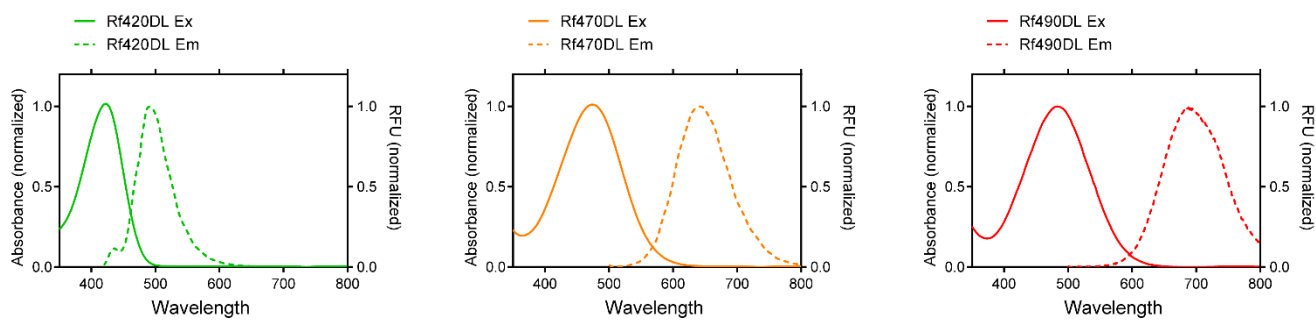
#### **Supplementary Movie 2.**

Time-lapse microscopy of PG synthesis in *B. subtilis* using **Rf470DL**. The cells were imaged in a cavity slide filled with LB-agarose (1.5%, w/v) containing 0.5 mM **Rf470DL**. The imaging was carried out at 37 °C for 4 hours. Left: merged channel from phase contrast and fluorescence channels; right: fluorescence channel.

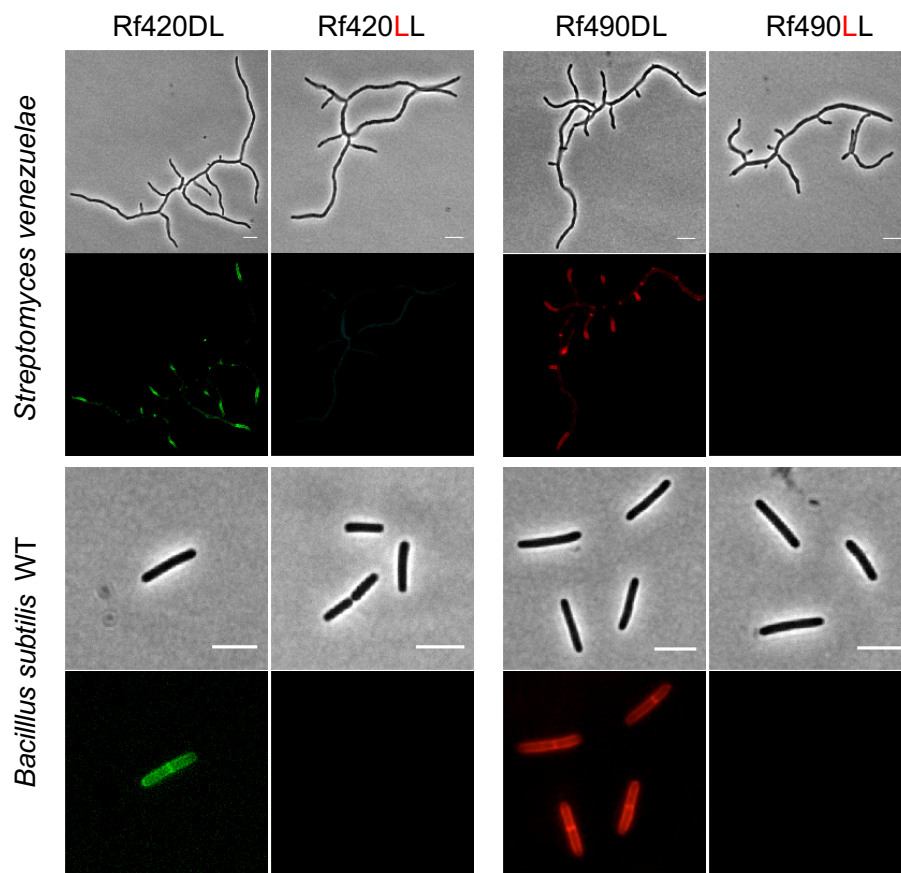
#### **Supplementary Movie 3.**

Time-lapse microscopy of PG synthesis in *B. subtilis* using **Rf470DL**. Non-growing cells became extremely fluorescent at a certain time point and then started lysis (at 02:12:00). The strong fluorescence might result from the entry of RfDAAs through the permeabilized membrane into the cytoplasm of the dead cell. The experiment was conducted under the identical condition as shown in **Supplementary Movie 2**. Left: merged channel from phase contrast and fluorescence channels; right: fluorescence channel.

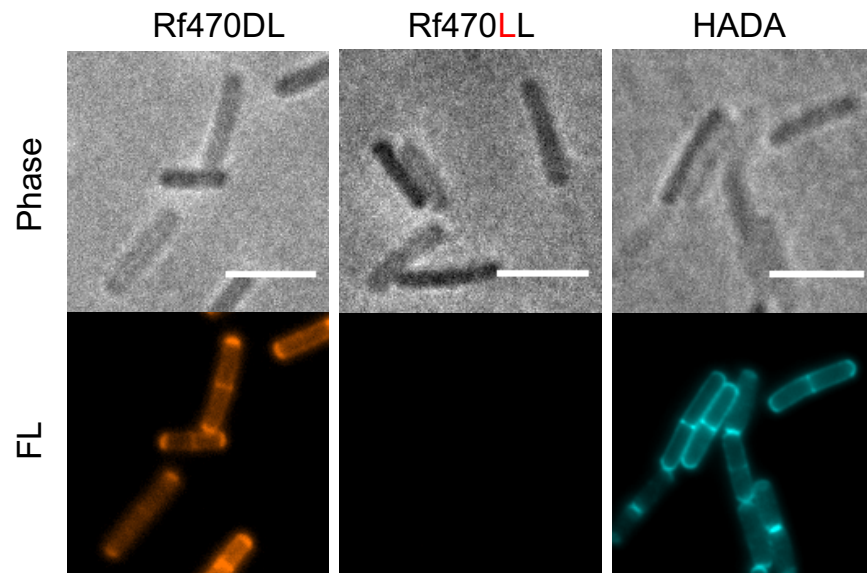
## SI-Figures



**Supplementary Fig. 1.** Excitation and emission spectra of RfDAAs. RfDAAs were dissolved in a 1:1 mixture of 1X PBP (pH 7.4) and glycerol to a final concentration of 0.1 mM. The measurements were carried out at 25 °C.

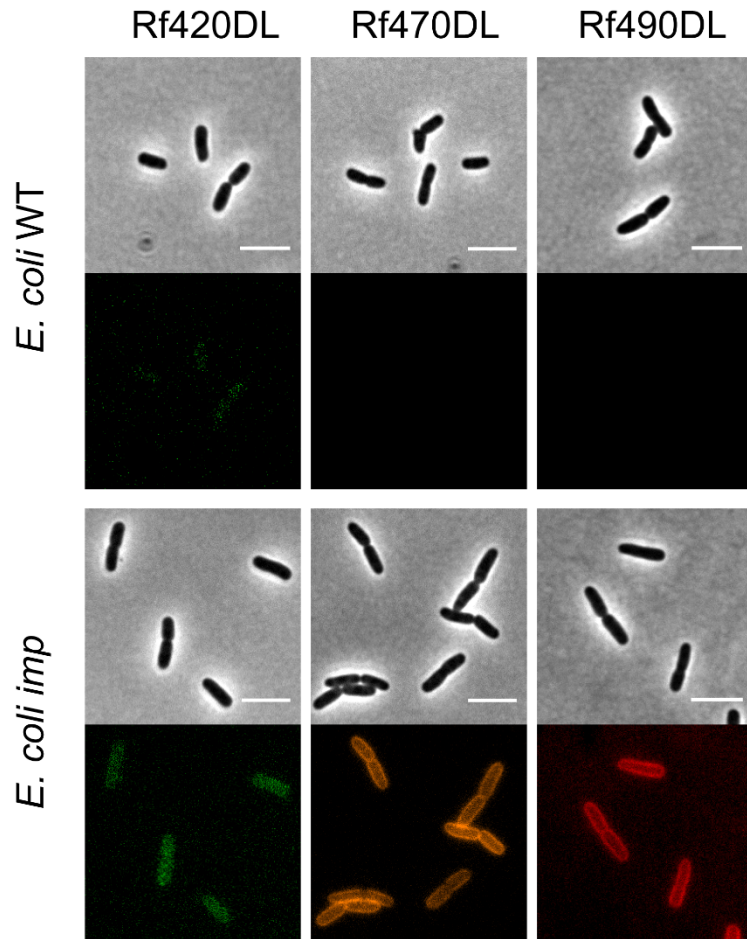


**Supplementary Fig. 2.** End-point imaging of RfDAA labeling in *S. venezuelae* (top, 15 min) and *B. subtilis* (bottom, 1 hour). Phase contrast channel was shown in the upper row; fluorescence channel was shown in the bottom row of each panel. Cells were imaged without washing and fixation. Identical labeling, imaging and processing conditions were used for the comparison between D- and L-enantiomers. Scale bar: 5  $\mu$ m.

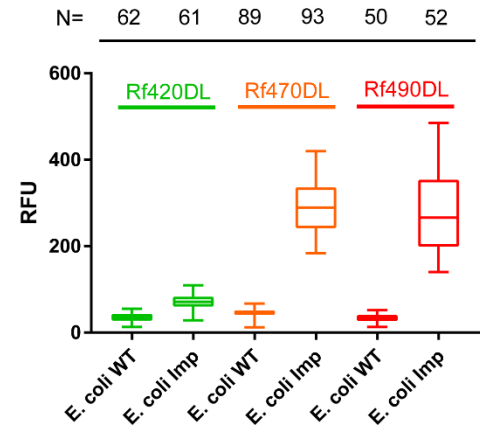


**Supplementary Fig. 3.** Isolated sacculi from *B. subtilis* labeled with **Rf470DL**, **Rf470LL** or **HADA**. Phase contrast channel was shown in the upper row; fluorescence channel was shown in the bottom row. Identical imaging and processing conditions were used for the comparison between D- and L-enantiomers. The L-enantiomers of RfDAA doesn't label PG because of the stereo-selectivity of PBPs. Scale bar: 5  $\mu$ m.

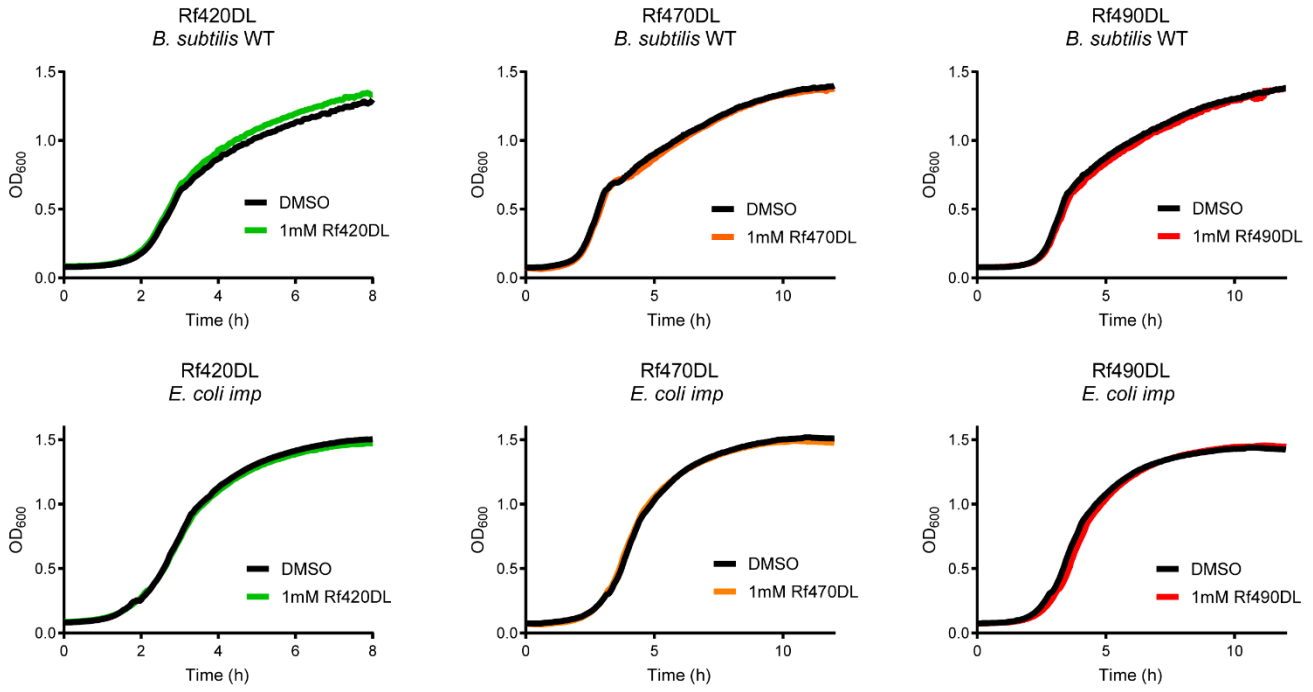
a



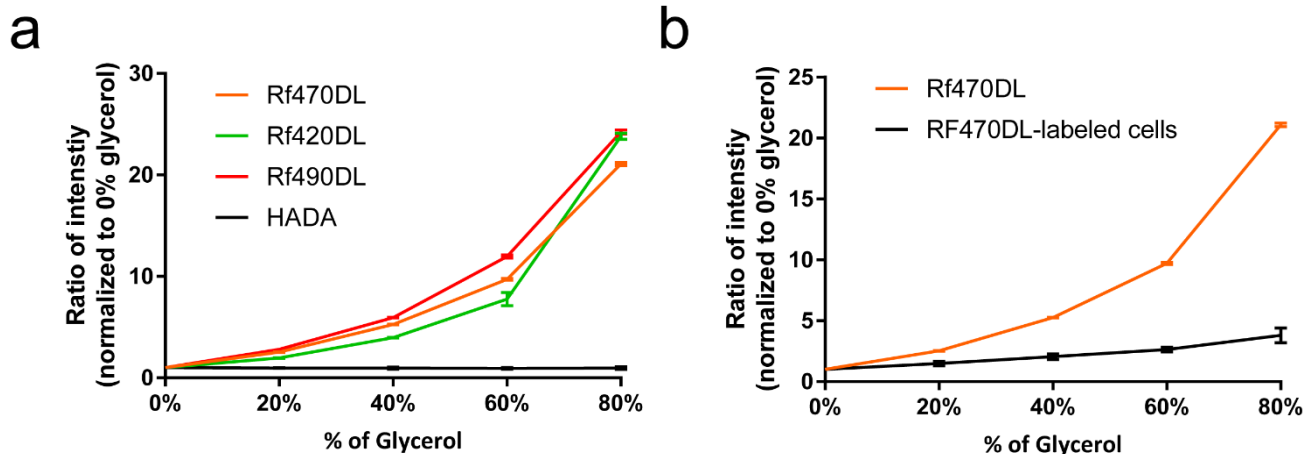
b



**Supplementary Fig. 4.** Comparison of RfDAA labeling between *E. coli* WT and *E. coli imp*. a) End-point images of labeled and fixed cells (1 hour labeling, 1 mM). No significant signal above the background was observed in *E. coli* WT with all RfDAA probes. **Rf470DL** and **Rf490DL** shown improved signal in *E. coli imp*. b) Quantification of fluorescence intensity of cells from A. Box-and-whisker plot: central line, median; box ends, upper and lower quartiles; whisker: upper and lower extremes. Background fluorescence was subtracted before the calculation. Identical labeling, imaging and processing conditions were used for the comparison. Scale bar: 5  $\mu$ m.

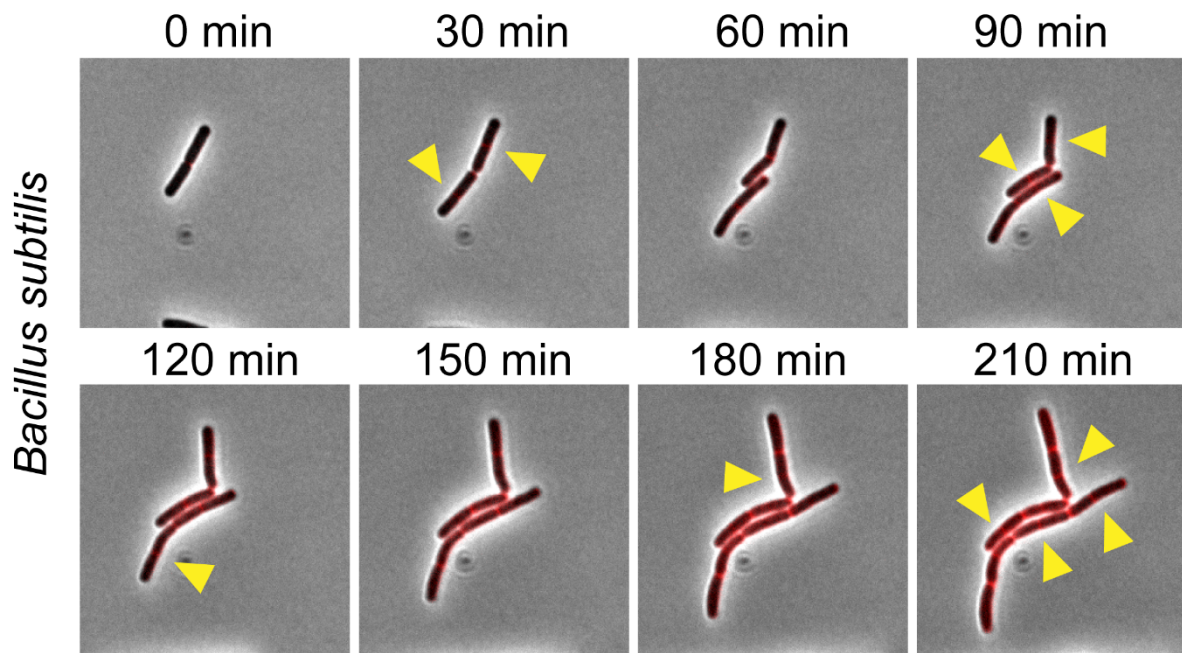


**Supplementary Fig. 5.** Growth curve measurement of *B. subtilis* WT and *E. coli imp* with or without RfDAAs.

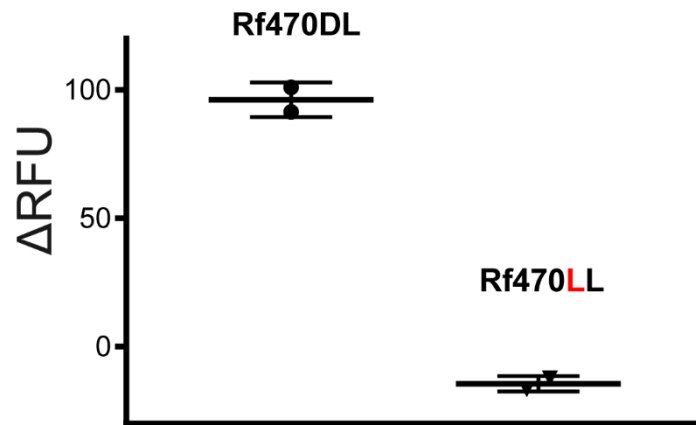


**Supplementary Fig. 6.** a) Comparison of viscosity sensitivity between RfDAAs and HADA. The fluorescence intensity of RfDAAs are sensitive to solvent viscosity but that of HADA is not. b) Comparison of viscosity sensitivity between free **Rf470DL** (from a) and PG-incorporated **Rf470DL** (*B. subtilis* cells labeled with **Rf470DL** for 1 hour). Cells were fixed with 70% ethanol for 1 hour and washed twice with 1X PBS before the measurements. **Rf470DL**-labeled cells showed reduced viscosity sensitivity with a calculated  $\chi$  value of 0.27. The data points were normalized to the 0% glycerol sample. Error bars: standard deviation.

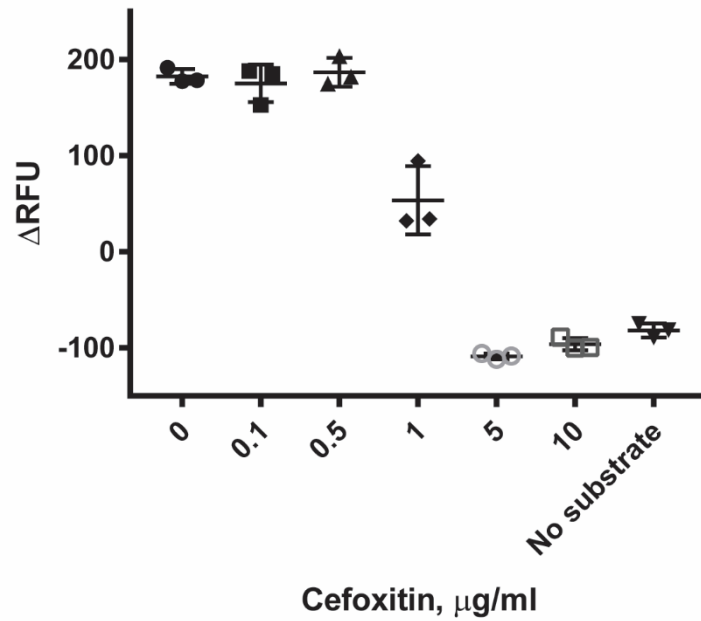




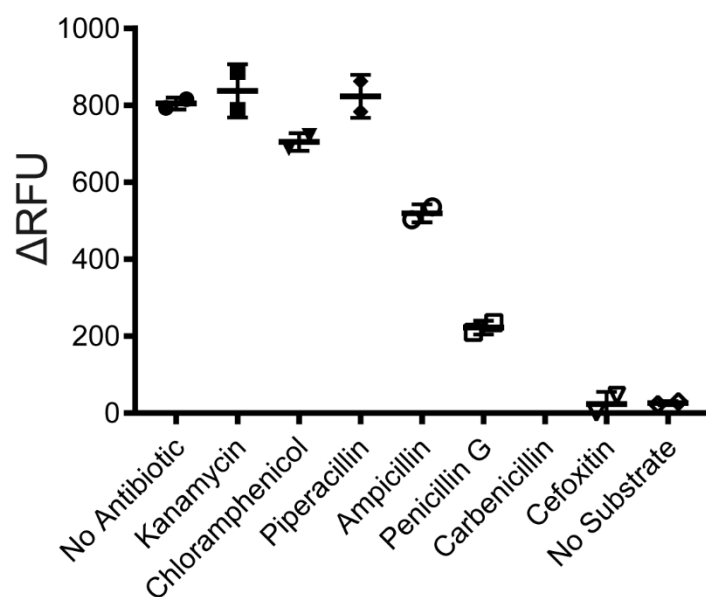
**Supplementary Fig. 7.** Montage of time-lapse micrographs of PG synthesis in live *B. subtilis* labeled with **Rf470DL**. Shown here are merged images from phase contrast and fluorescence channels. Arrowheads point out newly-made division septa. Also see Supplementary Movie 2.



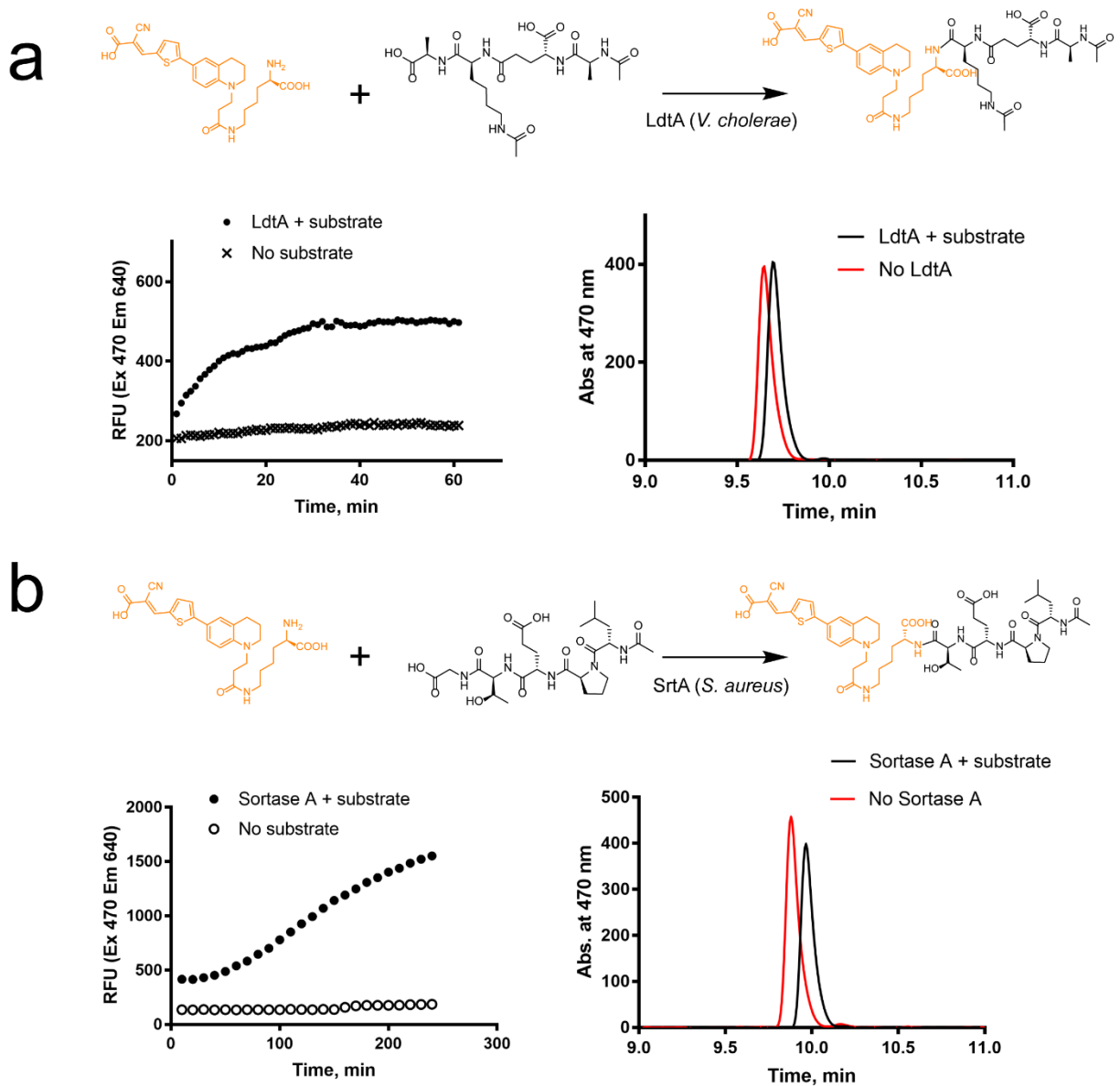
**Supplementary Fig. 8.** End-point assay of *S. aureus* PBP4 transpeptidase activity using **Rf470DL** and **Rf470LL**.  $\Delta$ RFU was calculated using the initial (T=0) and final (T= 1hour) fluorescence intensity of **Rf470DL**. No transpeptidase activity was observed when the L-enantiomer of RfDAA was used, confirming that the reaction was conducted by PBP activity which is specific to amino acids with D-chiral center. Error bars: standard deviation.



**Supplementary Fig. 9.** Cefoxitin dose-dependent assay on *S. aureus* PBP4. The enzyme activity was indicated by the intensity increase of Rf470DL upon incorporation into the tripeptide substrate.  $\Delta\text{RFU}$  presents the intensity change between the initial time point (T=0) and final time point (T=1 hour). The “No substrate” sample serves as the negative control for the experiment. An total inhibition was observed at the concentration of 5  $\mu\text{g/ml}$ .

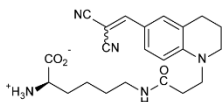


**Supplementary Fig. 10.** End-point study of antibiotic inhibition effect on *S aureus* PBP4 activity. The results of this end-point assay are consistent with the results obtained using initial rate measurements (Fig. 4). Data shown here are end-point values from a 1-hour reaction.  $\Delta$ RFU presents the intensity change between the initial time point (T=0) and final time point (T=1 hour). Antibiotics that do not interact with PBPs (off-targets) did not show inhibitory effect on the assay; whereas  $\beta$ -lactam PBP inhibitors shown inhibitory effects at different level. Bars: mean value and standard deviation.



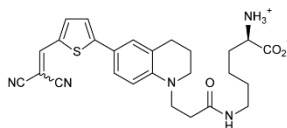
**Supplementary Fig. 11.** *In vitro* transpeptidation assays using **Rf470DL** and a) LdtA (*L,D*-transpeptidase, *V. cholerae*) or b) SrtA (Sortase A, *S. aureus*). Top: reaction schemes of the assays. Synthetic peptide substrates were used in the assays. Bottom left: real-time measurements of **Rf470DL** fluorescence intensity using a plate reader. The synthetic peptide substrates were either added or not to the reactions. Bottom right: cross-linked products from the assays were confirmed by HPLC. The enzymes were either added or not to the reactions.

a



**Rf460DL**

(malononitrile derivative of Rf420DL)

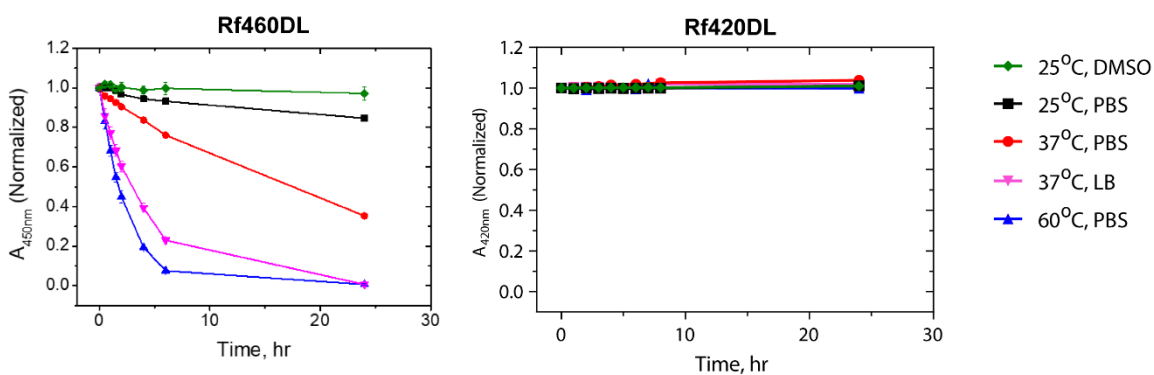


**Rf540DL**

(malononitrile derivative of Rf470DL)

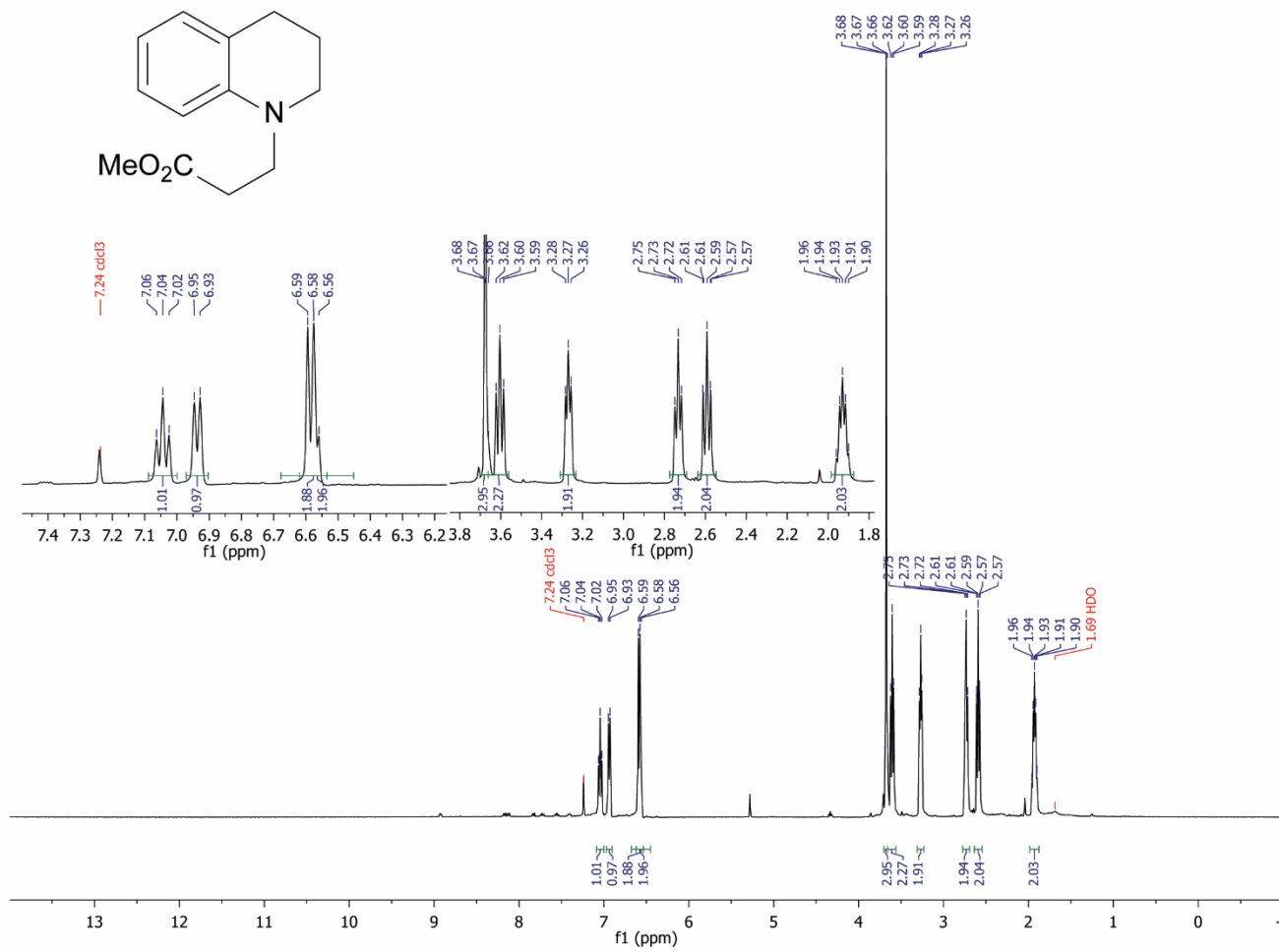
	<b>Rf460DL</b>	<b>Rf540DL</b>
MW (unsalted)	409.5	491.6
Max. $\lambda_{Ex}$	460	540
Max. $\lambda_{Em}$	500	660
Viscosity sensitivity ( $\chi$ )	0.623 $\pm$ 0.073	NA
Absorptivity ( $\epsilon$ )	12828	NA
Water-solubility (Log D <sub>7.4</sub> )	-0.251 $\pm$ 0.055	1.567 $\pm$ 0.106
Thermo-stability	13.5 $\pm$ 2.4%	NA

b

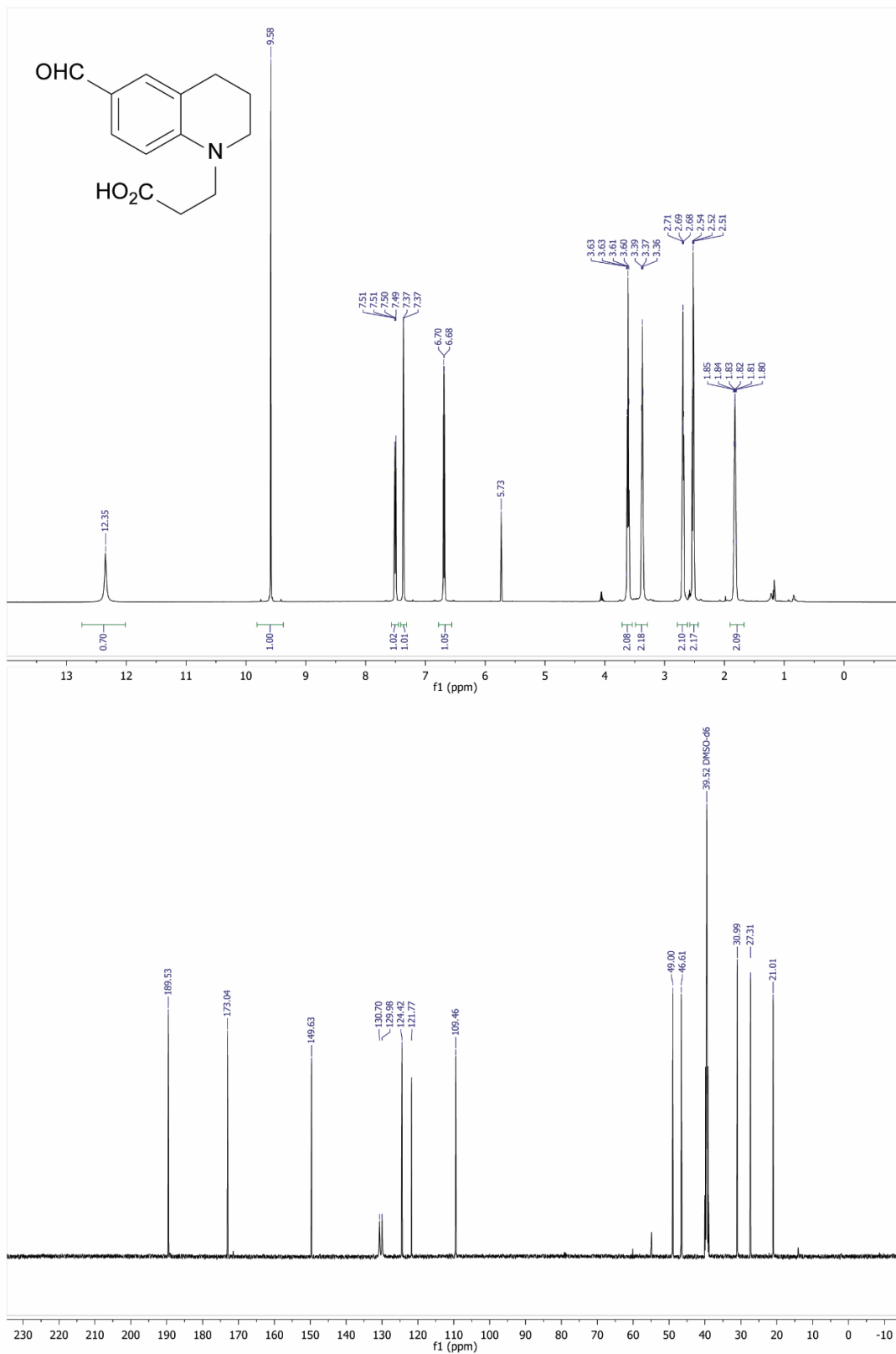


**Supplementary Fig. 12.** a) Structure of malononitrile derivatives of RfDAAs and their photochemical properties. NA: not applicable. The values were measured using the methods described in Table 1. b) Thermostability test of **Rf460DL** (left) and **Rf420DL** (right). **Rf470DL** and **Rf490DL** shown similar results with **Rf420DL** (data not shown). Test of **Rf540DL** is not available due to its poor water-solubility. Error bars: standard deviation.

## SI-NMR spectra

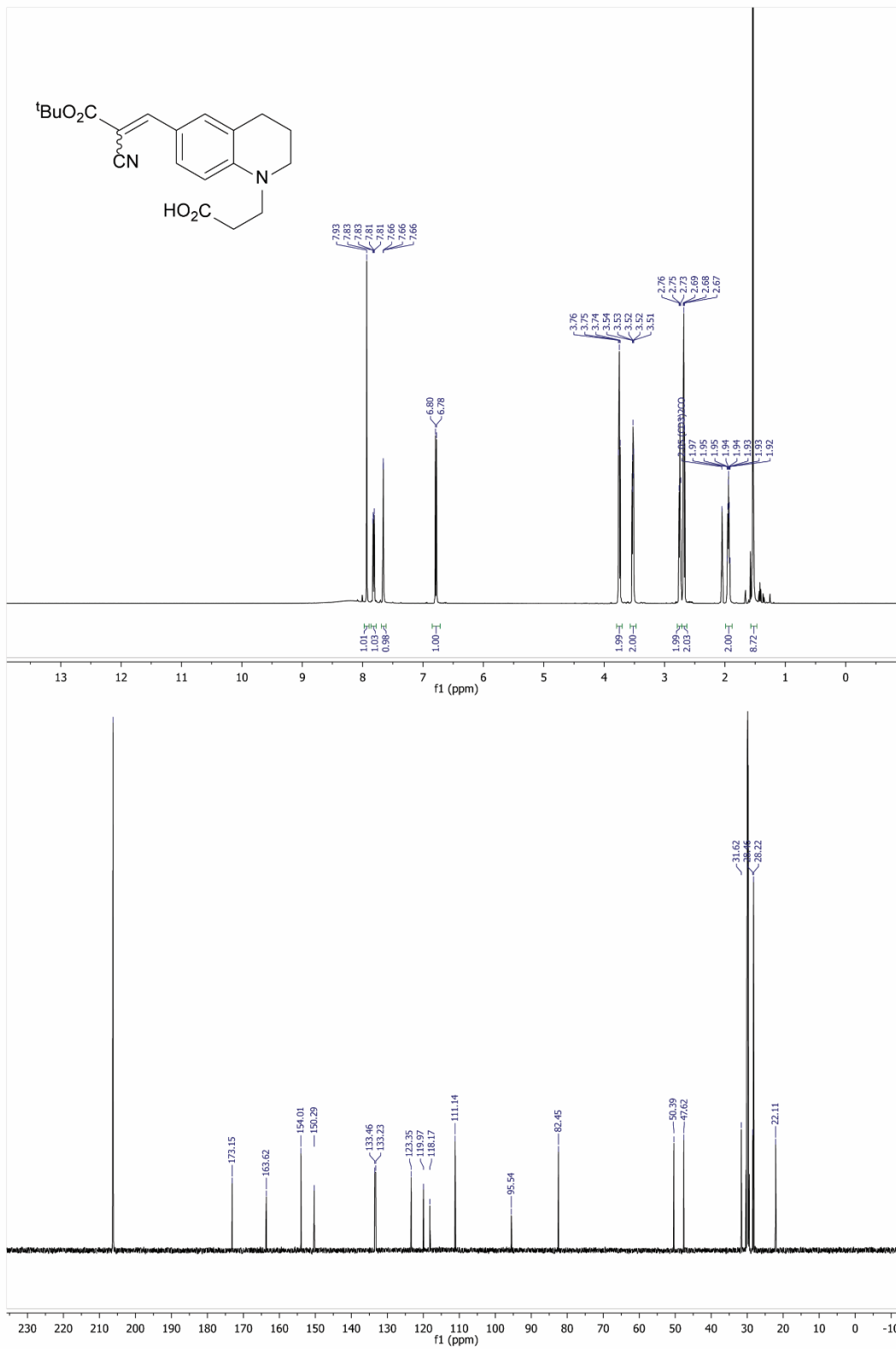


<sup>1</sup>H NMR of 1

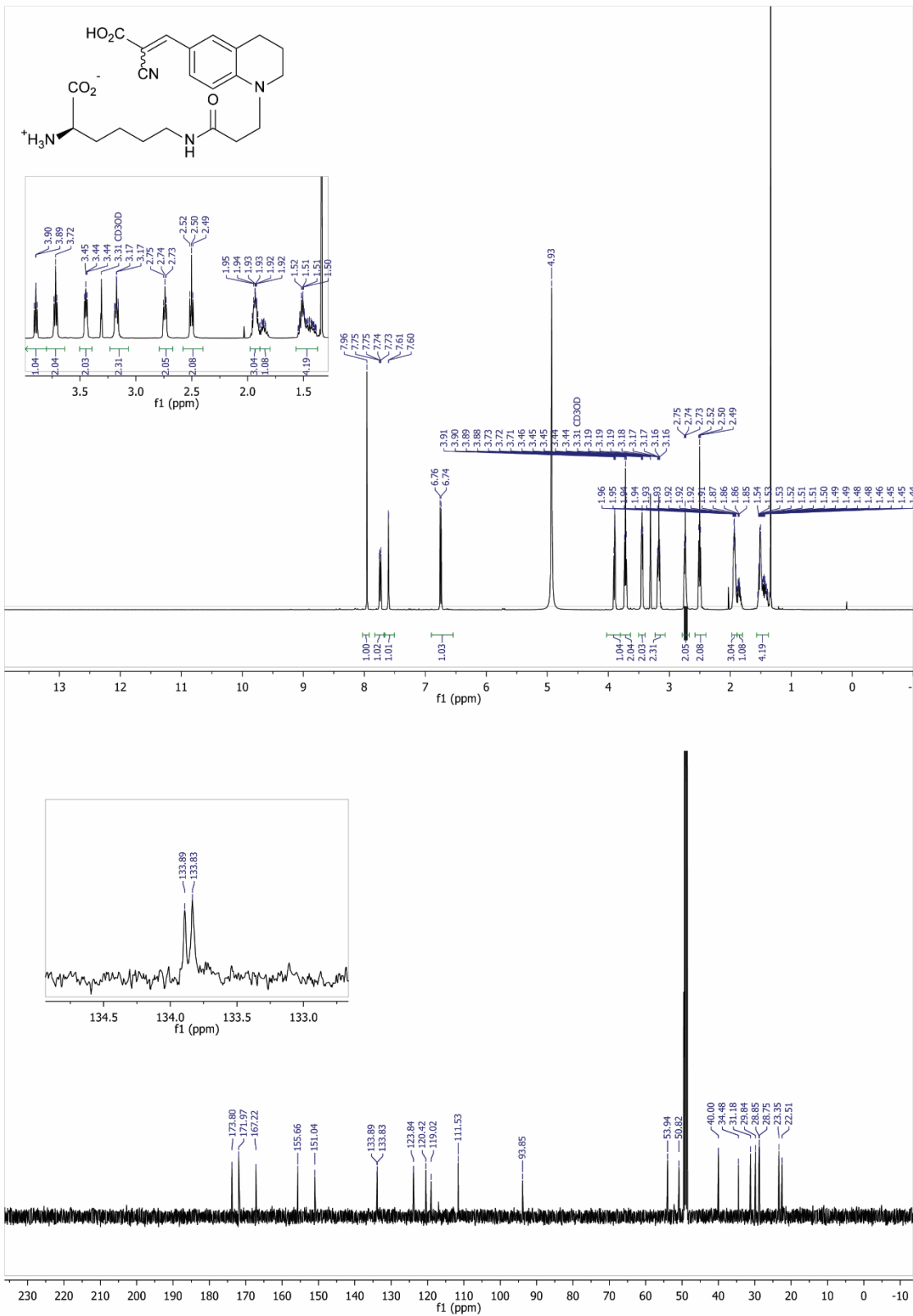


<sup>1</sup>H and <sup>13</sup>C NMR of 2

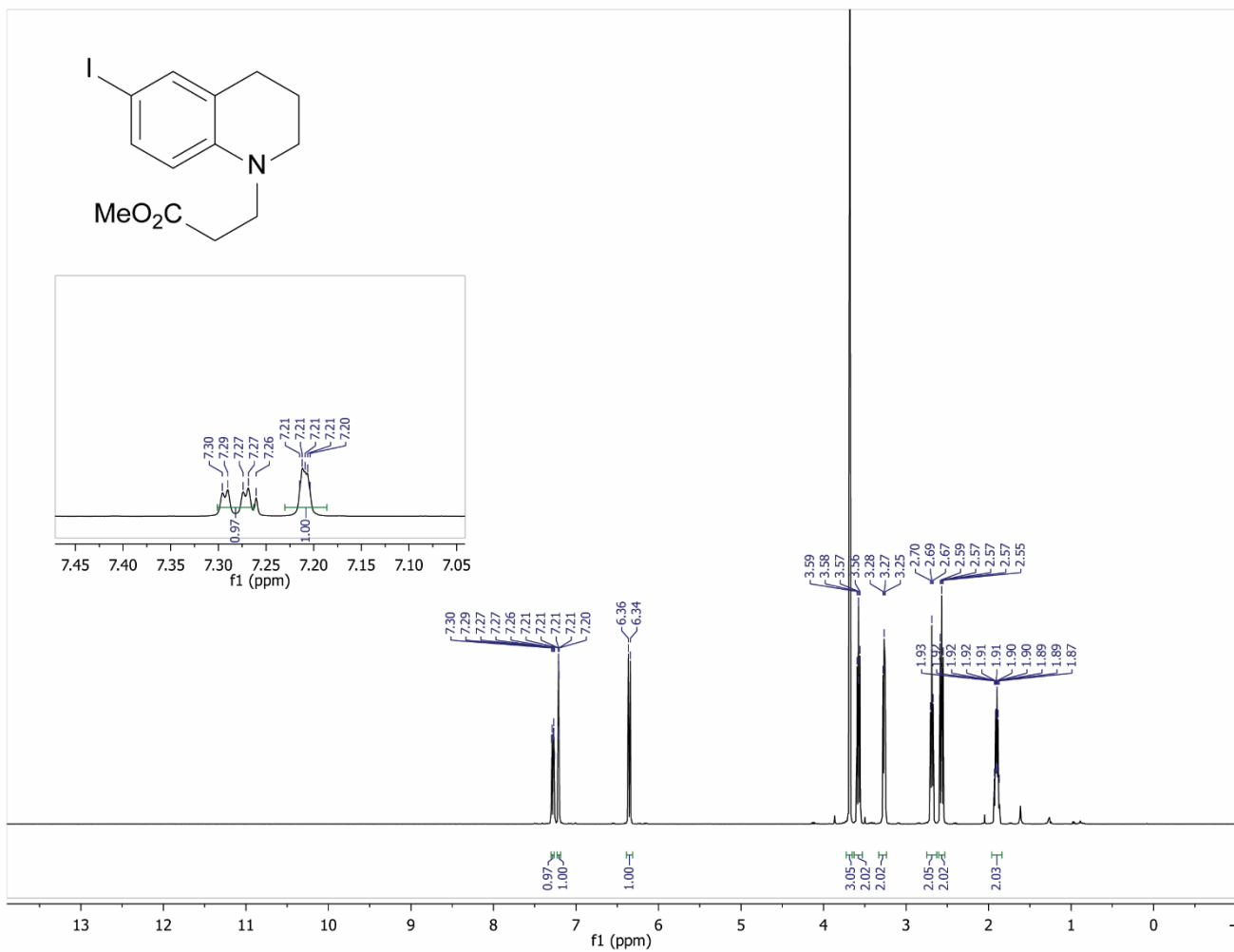




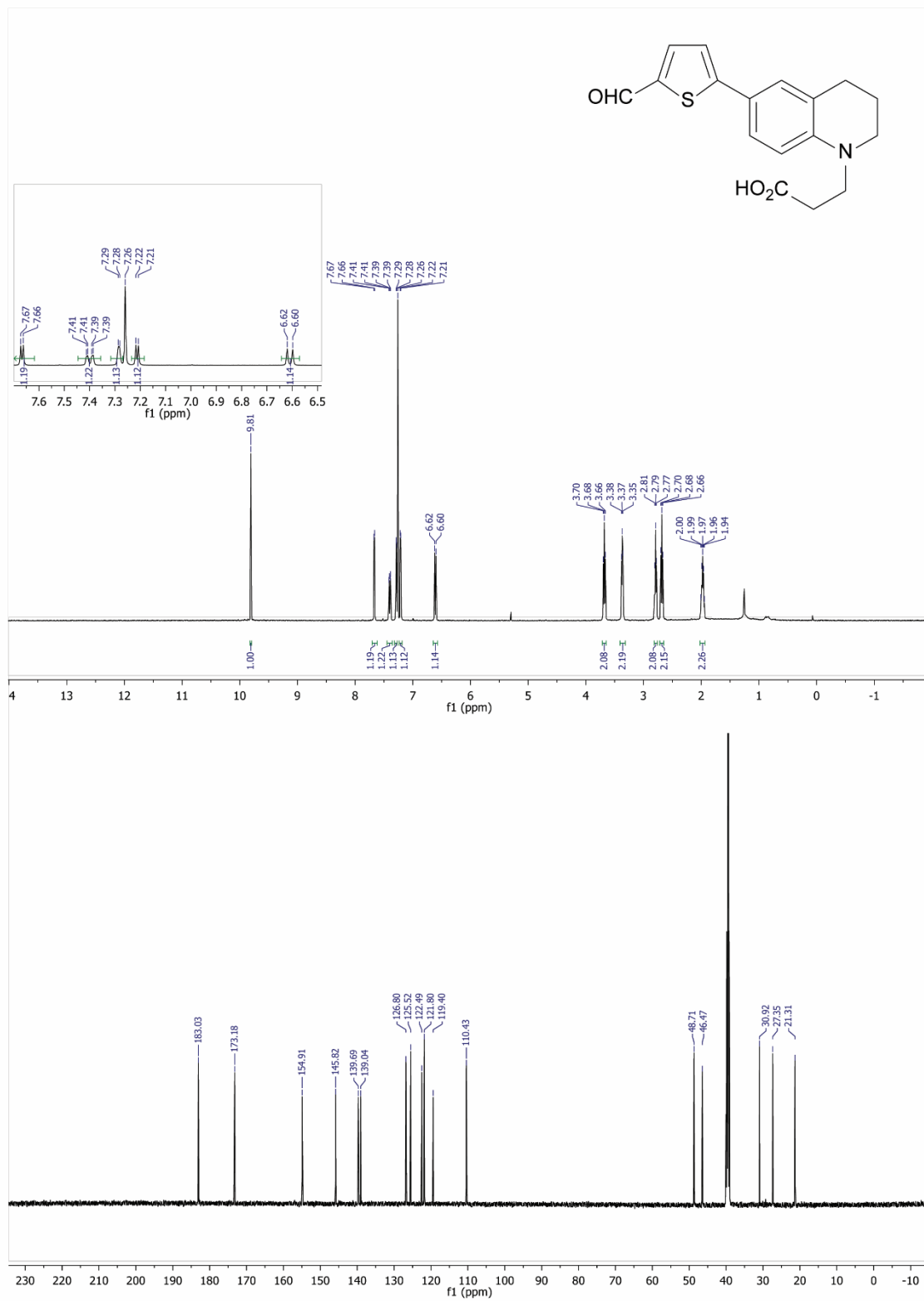
<sup>1</sup>H and <sup>13</sup>C NMR of 3



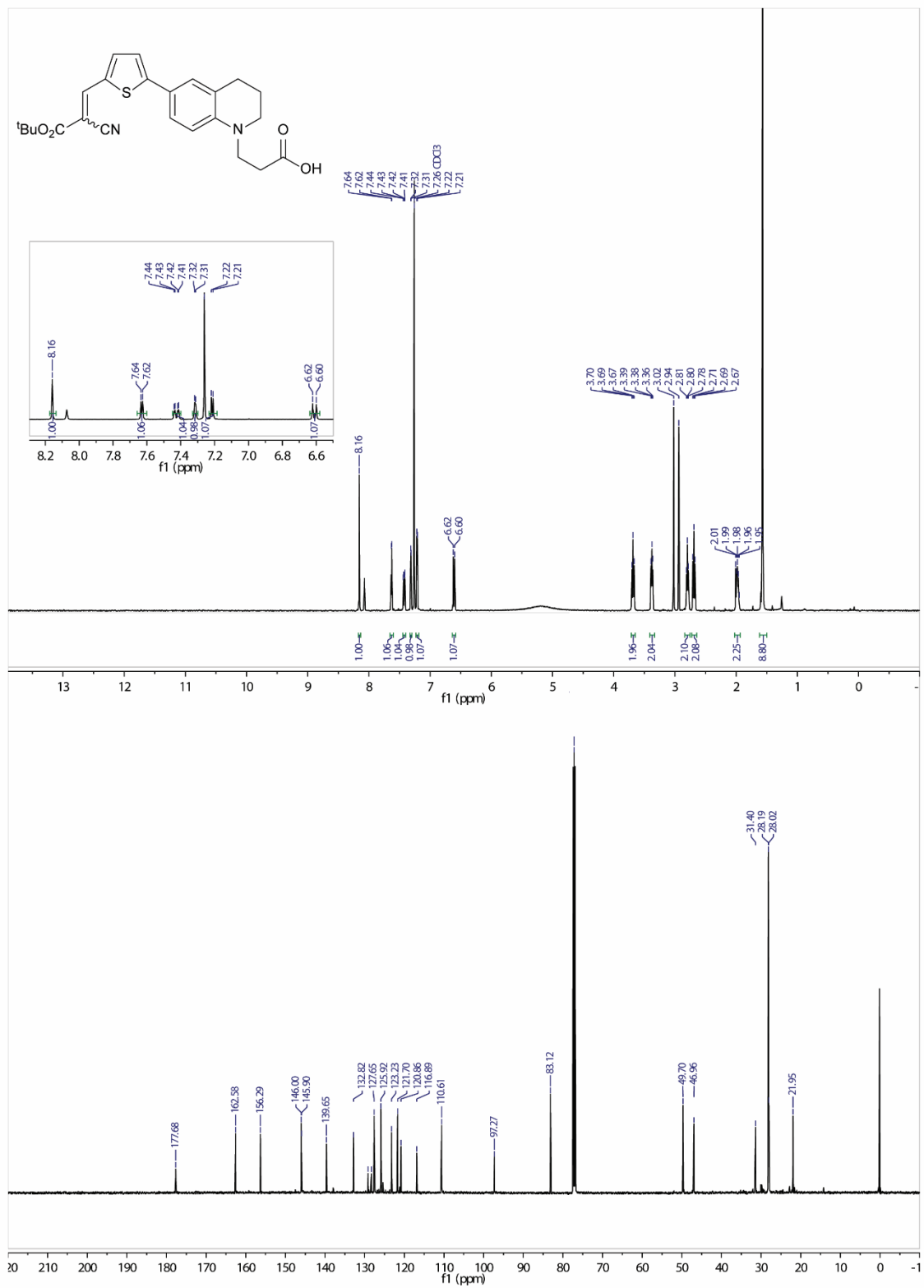
<sup>1</sup>H and <sup>13</sup>C NMR of Rf420DL



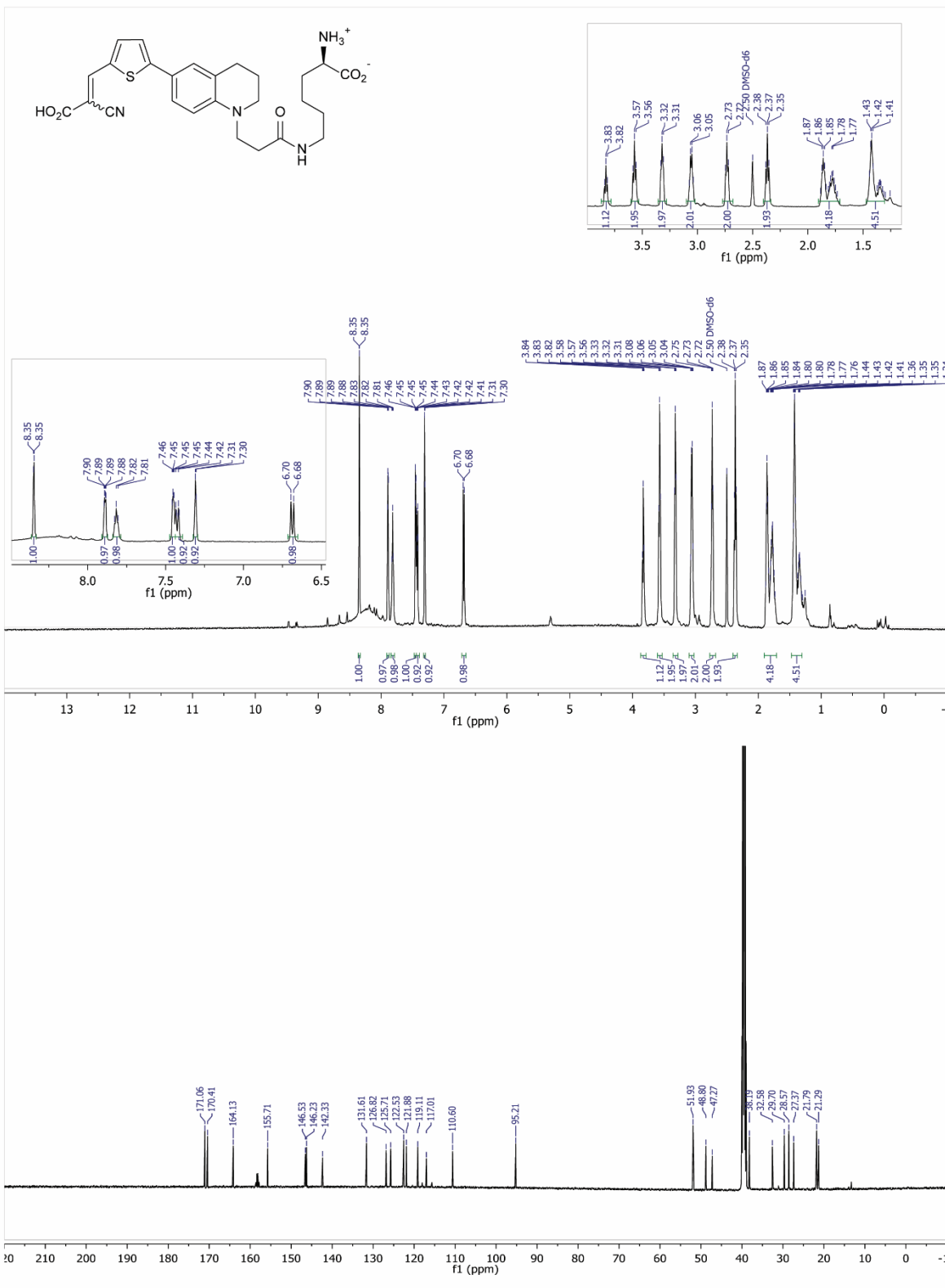
$^1\text{H NMR}$  of **4**



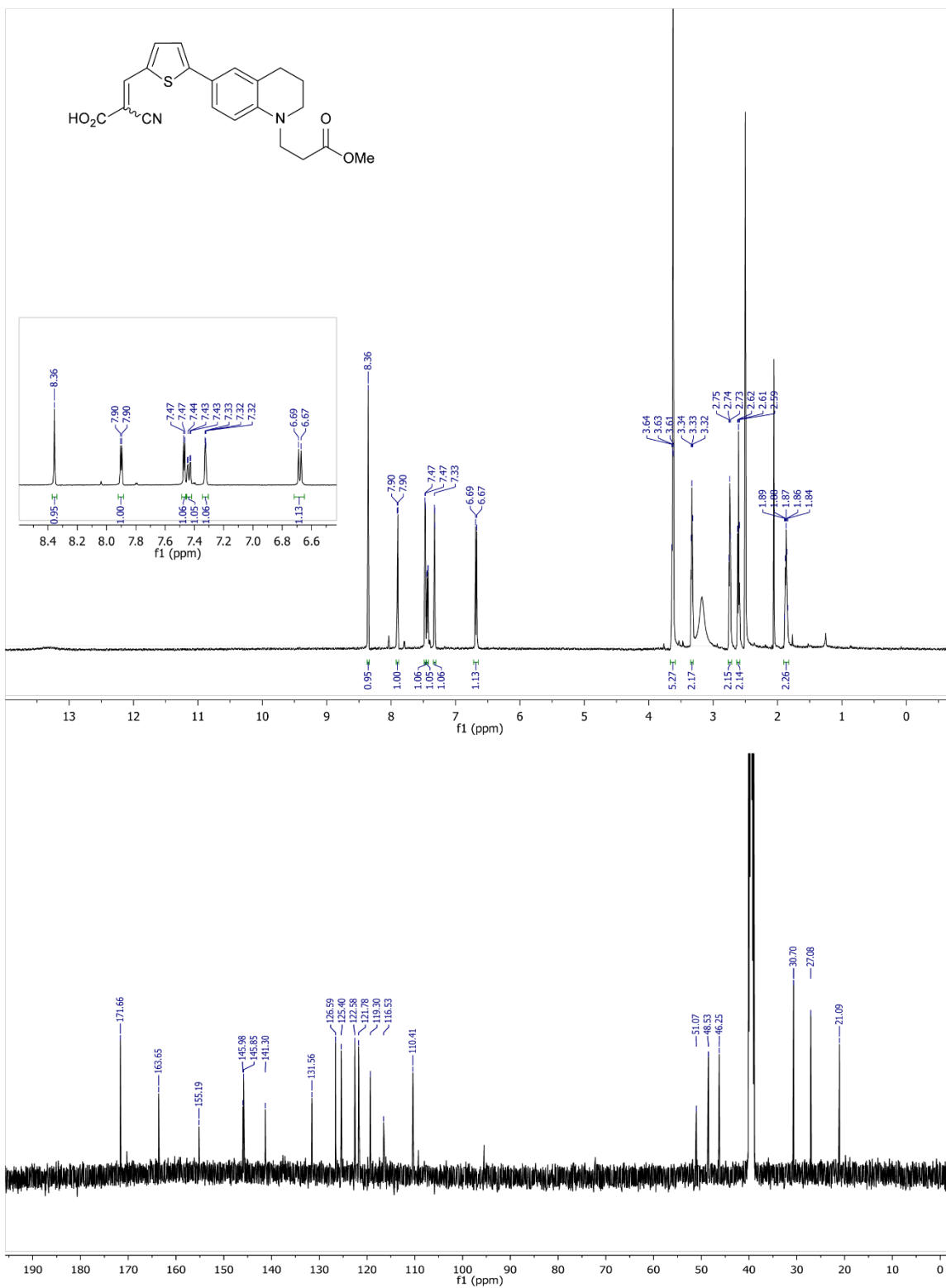
<sup>1</sup>H and <sup>13</sup>C NMR of 5



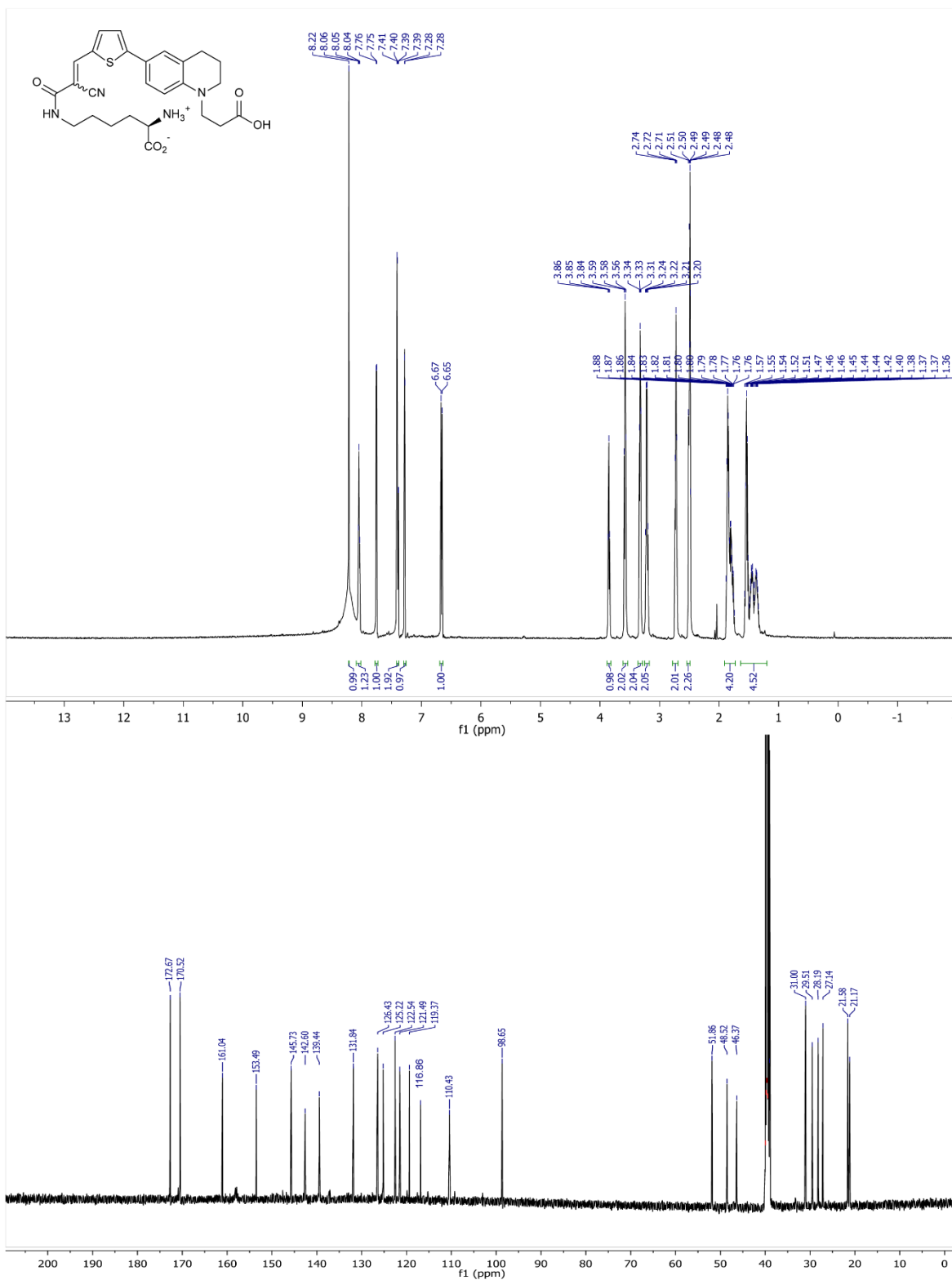
<sup>1</sup>H and <sup>13</sup>C NMR of **6**



**<sup>1</sup>H and <sup>13</sup>C NMR of Rf470DL**



<sup>1</sup>H and <sup>13</sup>C NMR of 7



**<sup>1</sup>H and <sup>13</sup>C NMR of Rf490DL**



## SI Table

**Supplementary Table 1. Bacterial strains used in this study**

<b>Species</b>	<b>Background</b>	<b>Source</b>	<b>#</b>	<b>Gram</b>	<b>Growth temperature</b>
<i>Bacillus subtilis</i> (WT)	3610	Brun Lab (IU)	YB7447	+	37
<i>Escherichia coli</i> (WT)	BW25113	Brun Lab (IU)	YB7421	-	37
<i>Escherichia coli</i> imp4213	BW25113	Huang Lab (Stanford)	KC440	-	37
<i>Streptomyces venezuelae</i> (WT)		Brun Lab (IU)	YB6837	+	30

## Reference

1. Sawada, S., Iio, T., Hayashi, Y. & Takahashi, S. Fluorescent rotors and their applications to the study of G-F transformation of actin. *Anal. Biochem.* **204**, 110–7 (1992).
2. Shao, J. *et al.* Thiophene-Inserted Aryl-Dicyanovinyl Compounds: The Second Generation of Fluorescent Molecular Rotors with Significantly Redshifted Emission and Large Stokes Shift. *European J. Org. Chem.* **2011**, 6100–6109 (2011).
3. Ducret, A., Quardokus, E. M. & Brun, Y. V. MicrobeJ, a tool for high throughput bacterial cell detection and quantitative analysis. *Nat. Microbiol.* **1**, 16077 (2016).
4. Lombardo, F., Shalaeva, M. Y., Tupper, K. A. & Gao, F. ElogDoct: A tool for lipophilicity determination in drug discovery. 2. Basic and neutral compounds. *J. Med. Chem.* **44**, 2490–2497 (2001).
5. Zhou, F. *et al.* Molecular Rotors as Fluorescent Viscosity Sensors: Molecular Design, Polarity Sensitivity, Dipole Moments Changes, Screening Solvents, and Deactivation Channel of the Excited States. *European J. Org. Chem.* **2011**, 4773–4787 (2011).
6. Cheng, N. S. Formula for the viscosity of a glycerol-water mixture. *Ind. Eng. Chem. Res.* **47**, 3285–3288 (2008).
7. Brouwer, A. M. Standards for photoluminescence quantum yield measurements in solution (IUPAC Technical Report). *Pure Appl. Chem.* **83**, 2213–2228 (2011).
8. Kuru, E. *et al.* In Situ probing of newly synthesized peptidoglycan in live bacteria with fluorescent D-amino acids. *Angew. Chem. Int. Ed. Engl.* **51**, 12519–23 (2012).
9. Qiao, Y. *et al.* Detection of lipid-linked peptidoglycan precursors by exploiting an unexpected transpeptidase reaction. *J. Am. Chem. Soc.* **136**, 14678–14681 (2014).
10. O'Callaghan, C. H., Morris, A., Kirby, S. M. & Shingler, A. H. Novel method for detection of beta-lactamases by using a chromogenic cephalosporin substrate. *Antimicrob. Agents Chemother.* **1**, 283–8 (1972).
11. Hsu, Y.-P. *et al.* Full color palette of fluorescent d -amino acids for in situ labeling of bacterial cell walls. *Chem. Sci.* **290**, 30540–30550 (2017).
12. Sangster, J. Octanol-Water Partition Coefficients of Simple Organic Compounds. *J. Phys. Chem. Ref. Data* **18**, 1111–1229 (1989).
13. Scherrer, R. A. & Howard, S. M. Use of distribution coefficients in quantitative structure-activity relationships. *J. Med. Chem.* **20**, 53–8 (1977).
14. Zgurskaya, H. I., López, C. A. & Gnanakaran, S. Permeability Barrier of Gram-Negative Cell Envelopes and Approaches To Bypass It. *ACS Infect. Dis.* **1**, 512–522 (2015).
15. Davis, T. D., Gerry, C. J. & Tan, D. S. General Platform for Systematic Quantitative Evaluation of Small-Molecule Permeability in Bacteria. *ACS Chem. Biol.* **9**, 2535–2544 (2014).
16. Haidekker, M. A. *et al.* New fluorescent probes for the measurement of cell membrane viscosity. *Chem. Biol.* **8**, 123–31 (2001).
17. Hawe, A., Filipe, V. & Jiskoot, W. Fluorescent molecular rotors as dyes to characterize polysorbate-containing IgG formulations. *Pharm. Res.* **27**, 314–26 (2010).